State-dependent Block of BK Channels by Synthesized Shaker Ball Peptides

Weiyan Li and Richard W. Aldrich

Section of Neurobiology, University of Texas at Austin, Austin, TX 78712

Crystal structures of potassium channels have strongly corroborated an earlier hypothetical picture based on functional studies, in which the channel gate was located on the cytoplasmic side of the pore. However, accessibility studies on several types of ligand-sensitive K^+ channels have suggested that their activation gates may be located near or within the selectivity filter instead. It remains to be determined to what extent the physical location of the gate is conserved across the large K^+ channel family. Direct evidence about the location of the gate in large conductance calcium-activated K^+ (BK) channels, which are gated by both voltage and ligand (calcium), has been scarce. Our earlier kinetic measurements of the block of BK channels by internal quaternary ammonium ions have raised the possibility that they may lack a cytoplasmic gate. We show in this study that a synthesized Shaker ball peptide (ShBP) homologue acts as a state-dependent blocker for BK channels when applied internally, suggesting a widening at the intracellular end of the channel pore upon gating. This is consistent with a gating-related conformational change at the cytoplasmic end of the pore-lining helices, as suggested by previous functional and structural studies on other K^+ channels. Furthermore, our results from two BK channel mutations demonstrate that similar types of interactions between ball peptides and channels are shared by BK and other K^+ channel types.

The Journal of General Physiology

INTRODUCTION

Much interest in the ion channel field surrounds the structure and properties of the pore, as it directly underlies the ultimate function of a channel—to allow ions to pass through. Very significant breakthroughs have been made in our understanding of ion channel pores with the solving of several K^+ channel structures (Doyle et al., 1998; Jiang et al., 2002a; Jiang et al., 2003; Kuo et al., 2003; Long et al., 2005). With a clear 3-D view of the selectivity filter of these K^+ channels, we now have a very thorough understanding of the mechanism for their selectivity for K^+ ions. Structures of the helices lining the wall of the channel pore have also provided important information about the geometry of the inner pore and cavity. Importantly, a vivid picture was proposed about the location of the channel gate and how it operates during the gating transition, based on the structures of two different prokaryotic K^+ channels (Doyle et al., 1998; Jiang et al., 2002a,b). However, in contrast to the very conserved signature sequence in the selectivity filter, the pore-lining helices share rather low sequence homology among different K^+ channels. It therefore remains to be determined how representative the available structural information in this region is across the large K^+ channel family. Functional studies have demonstrated that residues in the pore-lining helices have important influences on the biophysical properties of the channel pore such as gating, single channel conductance, sensitivity to blockers, and accessibility of modifying reagents (for example, Liu et al., 1997; Zei et al., 1999; del Camino et al., 2000; Ding and Horn, 2002, 2003; Hackos et al., 2002). These studies suggest that other than the selectivity filter, significant structural and functional variations likely exist in the remaining part of the channel pore among different K^+ channels.

A particularly important question in the studies of ion channels is the location of the channel gate. The majority of previous functional and structural studies on K^+ channels have suggested that the activation gate is located at the cytoplasmic end of the pore-lining helices (for review see Korn and Trapani, 2005). However, accessibility studies on several types of ligand-sensitive channels have provided evidences arguing for a different gate location (Flynn and Zagotta, 2001; Bruening-Wright et al., 2002; Proks et al., 2003; Xiao et al., 2003). Although the size of the cytoplasmic opening of the pore is known to be important for its conductance and pharmacology (Li and Aldrich, 2004; Brelidze and Magleby, 2005), direct evidence has been scarce either for or against a cytoplasmic gate in large conductance calcium-activated K^+ (BK) channels, which are gated by both voltage and calcium. In our earlier study using quaternary ammonium (QA) ions to probe the pore of BK channels (Li and Aldrich, 2004), we found that QA ions

Correspondence to Richard W. Aldrich: raldrich@mail.utexas.edu

Abbreviations used in this paper: BK, large conductance Ca^{2+}-activated potassium; C_{10}, decyltriethylammonium; EBP, enhanced ball peptide; QA, quaternary ammonium; ShBP, Shaker ball peptide; TBA, tetrabutylammonium.

have much faster on and off rates in BK channels when compared with other K^+ channels such as Shaker. In contrast to the effects of QA ions on other K^+ channels, block of macroscopic BK currents by QA ions doesn't demonstrate time dependence; and the deactivation of channels is not hindered by the presence of blocker. We interpreted our results as suggesting that the inner pore and the cavity of BK channels are larger than those of many other K^+ channel types. A less restricted diffusion can explain the fast kinetics of QA block, and the capacity of the cavity to readily trap the blocker can account for the lack of a "foot in the door" effect. However, as discussed in that study, another possible interpretation exists, in which the location of the BK channel gate differs from other K_v channels such that QA ions can freely access their binding site independently of the state of the gate. Because the kinetics of QA block is fast relative to the activation of BK channels, we were not able to conclusively distinguish between the two possibilities by establishing the dependence of the blockage on the state of the channel gate.

In this study we show that a much larger blocking molecule, a synthesized Shaker channel ball peptide (ShBP) homologue (enhanced ball peptide, or EBP), when applied from the intracellular side, results in block of BK channels with slow kinetics, allowing for analysis on the relative positions between the binding sites of the blocker and a channel gate. The sensitivity of BK channels to ShBP and its mutational homologues was discovered previously with single channel studies (Foster et al., 1992; Toro et al., 1992, 1994). The general consensus from these studies was that ShBPs inhibit BK channels in a similar mechanism as they do Shaker channels. However, previous kinetic analysis was complicated by the multi-exponential nature of single BK channel kinetics, and limited by the recording time. The state dependence of block by ShBPs in BK channels was not exclusively established. In light of the large quantitative differences in QA block of BK channels compared with other K^+ channels (Li and Aldrich, 2004), we now revisit the ShBP block with macroscopic K^+ currents carried by heterologously expressed BK channels. By establishing that ShBPs act on BK channels in the open-channel-block mechanism, we show in this study that the cytoplasmic end of the pore widens significantly upon channel opening. Consistent with the predicted gating transition by a cytoplasmic gate, this conformational change either represents the actual activation gating itself, or at least has significant influence on the conductance of BK channels. We also study further the electrostatic and hydrophobic interactions between the peptides and BK channels that are critical for binding. These findings complement the previous hypothesis that BK channels have conserved peptide binding mechanisms when compared with other K^+ channels such as Shaker (Foster et al., 1992; Toro et al., 1992, 1994).

MATERIALS AND METHODS

Channel Expression

All experiments were performed with *Xenopus laevis* oocytes injected with cRNA for different channel constructs. For appropriate levels of expression, 0.5–5 ng of cRNA was injected into each oocyte. Wild-type BK channels were the mbr5 clone of the mouse homologue of the *slo* gene (*mslo*) (Butler et al., 1993). The clone was modified and transcribed into cRNA as previously described (Cox et al., 1997). The E321N, E324N double mutant was a gift from C. Miller (Brandeis University, Waltham, MA). In some experiments this construct carried an unexpected point mutation (F395S), which had no discernible functional consequences compared with the construct with F395, based on all of our measurements. These results were therefore included in the statistical analysis. The S6/2-KcsA construct was generated by K. Hogan. 15 residues in the second half of the S6 domain in the BK channel (L_{312}AMFASYVPEIIELI$_{326}$) were replaced by the corresponding sequence in the inner helix of the KcsA channel (I_{100}TSFGLVTA-ALATWF$_{114}$) based on sequence alignment (Doyle et al., 1998). For this construct, site-directed mutagenesis was employed to introduce silent restriction sites to facilitate the insertion of a synthesized oligo nucleotide carrying the mutation. The final construct was verified by sequencing. For experiments with Shaker channels ShB Δ6-46 cRNA was injected into oocytes. Recordings were usually performed within 3–7 d after injection.

Electrophysiology

All recordings were performed in the inside-out patch clamp configuration (Hamill et al., 1981). Electrodes made from VWR borosilicate micropipettes (VWR Scientific) were coated with wax (Sticky Wax; Kerr Corporation) and fire polished before use. Pipette access resistance in the bath solution was between 0.8 and 1.5 MΩ so that the estimated voltage errors due to series resistance with largest currents were <10 mV and not corrected. All experiments were performed at 22°C.

Data acquired with an Axopatch 200-A patch clamp amplifier (Axon Instruments) were low-pass filtered at 10 kHz with its 4 pole Bessel filter. The ITC-16 hardware interface (Instrutech Scientific Instruments) and Pulse acquisition software (HEKA Electronik) were used to sample the records (at a 20-μs interval for macroscopic currents and 10 μs for single channels) and store data in a Macintosh G3 computer system. Unless otherwise indicated, capacitive transients and leak currents were subtracted from macroscopic currents via the use of a P/4 leak subtraction protocol with a leak holding potential of −120 mV. Four to eight consecutive current series under identical conditions were usually averaged before analysis to increase the signal to noise ratio. Experiments with visible time-dependent rundown of currents or kinetic changes were excluded from analysis. Single channel analysis was performed with the QUB software (Qin et al., 1996) as previously described (Li and Aldrich, 2004). Statistical analysis, graphing, and curve fitting were performed with Igor Pro Software (WaveMetrics Inc.). Nonlinear least-squared fits were performed using the Levenberg-Marquardt algorithm. Modeling was performed using an Igor Pro routine written by F. Horrigan (Horrigan et al., 1999).

Solutions

Pipette (extracellular in inside-out configuration) solution contained (in mM) 140 $KMeSO_3$, 20 HEPES, 2 KCl, and 2 $MgCl_2$ (pH 7.20); bath (intracellular) solution: 136 $KMeSO_3$, 20 HEPES, 6 KCl, and 0.1 $CaCl_2$ (pH 7.20). In the absence of added Ca^{2+} buffer, 0.1 mM added $CaCl_2$ in the bath solution resulted in a free Ca^{2+} concentration of 110 μM, as measured with a Ca^{2+} electrode (Orion Research Inc.) (Bers, 1982). This solution is referred to as "High Ca^{2+}" solution in the text. High Ca^{2+} solution was used in

all experiments except in some cases where a low Ca^{2+} internal solution was used for lower open probability. For this solution, 5 mM HEDTA and 0.99 mM $CaCl_2$ were added into the intracellular solution. The free Ca^{2+} concentration in this low Ca^{2+} solution was measured to be 0.85 μM with the Ca^{2+} electrode. This solution is referred to as "Low Ca^{2+}" solution in the text. Contaminant Ba^{2+} was chelated by 40 μM (+)-18-crown-6-tetracarboxylic acid (18C6TA), added to the internal solution just before experiments (Diaz et al., 1996; Neyton, 1996; Cox et al., 1997). 18C6TA also chelates Ca^{2+}; therefore the actual free Ca^{2+} concentration in the unbuffered High Ca^{2+} solution was lower than 110 μM. On the other hand, the effect of 18C6TA on the free Ca^{2+} concentration of the Low Ca^{2+} solution should be small due to excessive HEDTA. The application of solutions was controlled by a sewer pipe flow system (DAD-12; Adams and List Assoc. Ltd.) as previously described (Li and Aldrich, 2004).

Chemicals

ShBP (MAAVAGLYGLGEDRQHRKKQ) and EBP (MAAVAGLYGLGKKRQHRKKQ) were synthesized and HPLC purified by the Protein and Nucleic Acid Facility at Stanford University. All peptides were acetylated on the N terminals and amidated on the C terminals to eliminate charged atoms at the ends. Peptide products were assumed 100% pure for calculating the concentrations. Tetrabutylammonium (TBA) was obtained from Alfa Aesar. Decyltriethylammonium (C_{10}) was a gift from C. Armstrong (University of Pennsylvania, Philadelphia, PA). All other chemicals were ordered through Sigma-Aldrich.

RESULTS

Previously, the blockage of BK channels by synthesized ShBP was studied at the single channel level with natively expressed channels incorporated into bilayers (Foster et al., 1992; Toro et al., 1992). These studies revealed two kinetically distinct components of block: a frequent, short-duration (lifetime of ~10 ms) block with higher affinity, and a rarer, longer-lived (lifetime of ~100 ms) block with lower affinity. Correspondingly, it was proposed that ShBP produces block of BK channels in two distinct states. In this paper we refer to the two states as short and long blocks, respectively. When we apply ShBP to macroscopic K^+ currents carried by heterologously expressed BK channels, the time-dependent block also routinely manifests two exponential components (Fig. 1 A). However, it's unlikely that these two components can be respectively accounted for by the previously characterized short- and long-lived block states. When roughly half of the channels are blocked, the time constants for the two components are ~2 ms and ~10 ms, respectively. Based on these time constants, estimates of average lifetime for both components fall into the range previously characterized as short blocks. Separation of the two components within the short block events was not previously identified, possibly due to the limited resolution in the dwell time distributions of single channel events, or due to variations among different BK constructs. Nevertheless, our macroscopic measurement agrees with the previous finding at the single channel level in that the majority of the block events are short lived when about half of the currents are blocked.

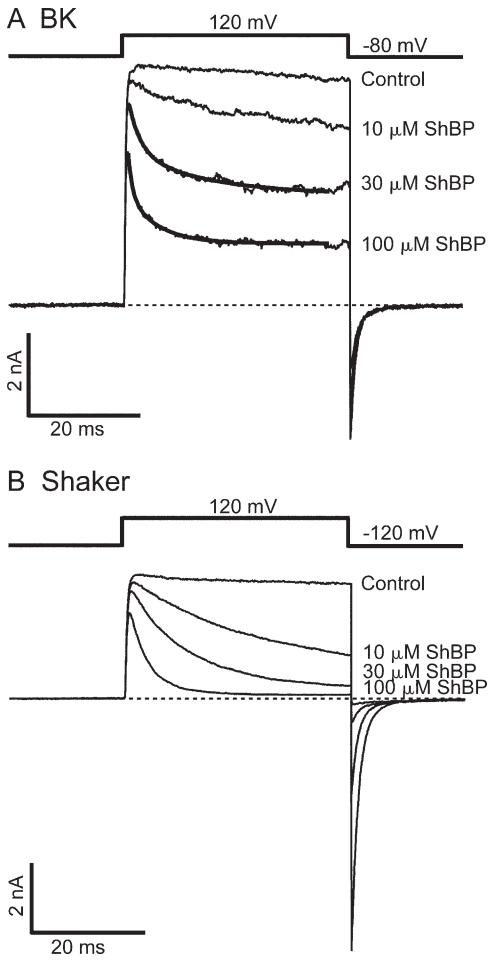

Figure 1. Time-dependent blockage of BK and Shaker currents by synthesized ShBP. (A) Macroscopic BK currents were recorded from an inside-out patch exercised from an oocyte expressing *mslo* construct. Currents elicited by the voltage protocol shown above were recorded under voltage clamp in the absence (control) and presence of 10, 30, and 100 μM ShBP. Currents in the presence of 30 and 100 μM ShBP were fitted with double exponential time course (thick smooth lines). Time constants in the fitting are τ_{fast}= 2.0 ms, τ_{slow}= 13.1 ms (30 μM), and τ_{fast}= 0.7 ms, τ_{slow}= 5.2 ms (100 μM). (B) Macroscopic Shaker currents were recorded from an inside-out patch exercised from an oocyte expressing ShB Δ6-46 construct. Recording conditions were the same as in A except for the holding potential of −120 instead of −80 mV. Macroscopic currents shown in this and other figures represent the average of four to eight consecutive traces unless otherwise noted. Dashed lines in this and other figures indicate zero current level for macroscopic currents.

The time course of BK currents in the presence of ShBP is reminiscent of the time-dependent block of Shaker K^+ currents by ShBP that has been exhaustively studied (Murrell-Lagnado and Aldrich, 1993a,b). For comparison to BK channel block we have recorded Shaker K^+ currents in response to ShBP under identical conditions (Fig. 1 B). In spite of much resemblance,

however, block of BK and Shaker currents by ShBP do have noticeable differences, with Shaker currents showing slower block and higher apparent affinity, suggestive of a slower apparent peptide dissociation rate. This observation is consistent with previous measurements of ShBP dissociation rate ($\sim$10 s^{-1}) in Shaker channels (Murrell-Lagnado and Aldrich, 1993b) and the dissociation rate for the short block of BK channels ($\sim$100 s^{-1}) (Foster et al., 1992; Toro et al., 1992).

A variant of ShBP in which the net charge was increased from +2 to +6 by two mutations (E12K, D13K) was found to have a significantly higher association rate for Shaker channels than native ShBP. With minimal effect on the dissociation rate, this variant has a much higher affinity for Shaker channels (Murrell-Lagnado and Aldrich, 1993b) (Fig. 2 B), and has been referred to as the "enhanced ball peptide" (EBP). Previously, EBP was also tested on single BK channels near 0 mV, and found to result in mostly short block events (Toro et al., 1994). EBP has a higher affinity for BK channels than ShBP, which was believed mainly due to an increase in the association rate. When EBP was applied to macroscopic BK currents at positive potentials (e.g., +120 mV), it resulted in obviously different responses than ShBP (compare Fig. 2 A with Fig. 1 A). In addition to a significant increase in apparent affinity, as consistent with previous single channel studies, the kinetics of EBP block also appears to be different from ShBP. In contrast to ShBP block, the time course of EBP block can be fitted well with a single exponential component (Fig. 2 A). Interestingly, the kinetics of EBP block in BK channels appears more similar to the block of Shaker channels by both ShBP and EBP. This suggests that EBP primarily results in a single block state in BK channels with longer lifetime, in contrast to ShBP. Indeed when low concentration of EBP blocks roughly half of the channels, the time constant of the single exponential decay is $\sim$100 ms (unpublished data). Assuming roughly equal apparent association and dissociation rates under this condition, such a value corresponds to an apparent dissociation rate of $\sim$5 s^{-1}, within the range of the long block events previously characterized in ShBP block of single BK channels (Foster et al., 1992). The dominance of long block events in the EBP block of BK channels at positive potentials can be illustrated by zooming in on the steady-state level when most of the macroscopic currents are blocked (Fig. 3 A). When steady state is reached in the presence of 3 μM EBP, single channel openings to the full current level are clearly evident. This is expected with a very slow dissociation rate because most channels stay in the long block state, with very low probability to unblock. Such an observation is not expected if fast block events primarily result in a nearly complete steady-state block, in which case we would see the ensemble of block and unblock events of a large number of channels, which won't be fully resolvable at the single channel level. Consistent with macroscopic measurements, single channel recordings of BK channels at 80 mV in the presence of 0.3 μM EBP demonstrated primarily block events lasting hundreds of milliseconds (Fig. 3 B), although direct kinetic measurements of long-lasting block with single channel recordings were limited by the time of recordings and complicated by the multiple modes of single BK channel kinetics (Silberberg et al., 1996).

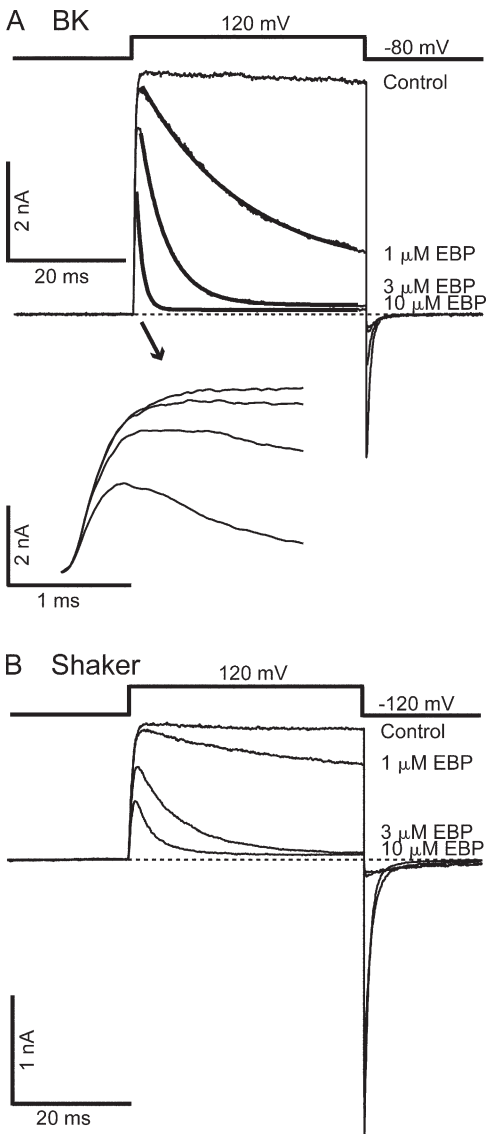

Figure 2. EBP demonstrates slower block and higher affinity than ShBP in BK channels. (A) Macroscopic BK currents recorded at 120 mV are shown in the absence (control) and presence of 1, 3, and 10 μM EBP. Currents in the presence of blocker are fitted with single exponential time course (thick smooth lines). Time constants in the fitting are τ = 17.6 ms (1 μM), τ = 4.5 ms (3 μM), and τ = 1.1 ms (10 μM). The first 2 ms of the currents during depolarization were amplified in the inset below to illustrate the activation. (B) Macroscopic Shaker currents recorded in the absence (control) and presence of 1, 3, and 10 μM EBP with the voltage protocol shown above the traces.

For the rest of the study we focus our interest on the block of BK channels by EBP, because its relatively slow time course helps our analysis on the state dependence of the block, in order to probe the location of BK channel gates relative to the peptide binding site. In an earlier study (Li and Aldrich, 2004), we showed that QA ions such as C_{10} and TBA result in the block of BK currents without apparent time dependence, raising the possibility that the QA binding site is accessible from the intracellular side even in a closed channel. Given the likelihood that ball peptides may bind to the channel near the QA binding site (Choi et al., 1991; Zhou et al., 2001), the slow block by EBP offers an opportunity to probe the relative position between these binding sites and the BK channel gate. The time course of the block by EBP immediately suggests that it can only block BK channels that are open, as do the classic open-channel blockers. Noticeably, the rising phase of BK currents in the presence of 1 μM EBP is largely unchanged compared with control (Fig. 2 A, bottom). As predicted by an open-channel-block mechanism, when the concentration of EBP is increased and the rate of block is higher, the peak current amplitudes are reduced because a significant number of channels are blocked before the activation of all channels would have reached steady state. This suggests that closed channels remain unblocked and are activated normally by depolarization, and can only be blocked after they are open.

Suggestive as it is, however, the time dependence of block itself does not exclusively prove an open-channel-block mechanism. For example, if the block is dependent on voltage, it is possible that the negative membrane potentials rather than the state of channels are the real reason why the channels are not blocked before depolarization. Similar cautionary consideration has been discussed for other blockers of K^+ channels (Clay, 1995). In fact, block of single BK channels by native ShBP and EBP was previously found to be voltage dependent (Foster et al., 1992; Toro et al., 1992, 1994). Our results with macroscopic BK currents also demonstrate that EBP block is clearly dependent on the membrane potential. In Fig. 4 (A–D), representative BK currents elicited by depolarization of membrane potentials between −80 and 160 mV are shown in the absence and presence of EBP at different concentrations. Higher concentrations of EBP and more depolarized membrane potentials result in faster time courses of the block and lower fractions of remaining currents at the end of the depolarizing pulses relative to the control currents. Fig. 4 E illustrates that the fraction of remaining current (I/I_o) at the end of 60-ms pulses in the presence of 1 μM EBP decreases with increased membrane potentials ($n = 6$). At positive voltages (≥40 mV), the inhibition of BK currents by EBP at all concentrations can be fitted well with a single exponential time course. The fitting of the decay starts at some point after the peak of currents. Under these recording conditions, BK channels have an open probability (P_o) near unity at equilibrium and the activation is faster compared with the current decay. We therefore assume that at this point BK channels are already fully opened, and the current decay after this purely reflects the block of open channels with no significant contribution from the Closed↔Open transition. This is supported by the fact that current decay can be fitted well with a single exponential time course. The reciprocals of the time constants

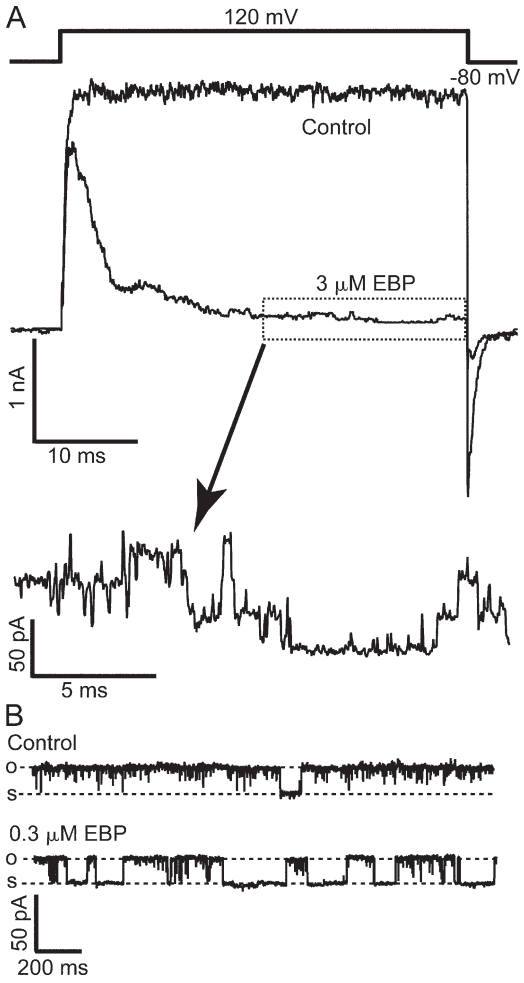

Figure 3. Steady-state block of BK channels by EBP is dominated by long block events. (A) Macroscopic BK currents were recorded before (control) and after the application of 3 μM EBP. Voltage protocol is shown above the traces. Currents were not leak subtracted nor averaged in order to demonstrate the unaltered single channel openings. The segment of current enclosed in the dotted box was amplified both vertically and horizontally to visualize single channel currents. (B) Single channel recordings of BK currents in the absence (control) and presence of 0.3 μM EBP at 80 mV. Records were digitally filtered at 1 kHz. Dashed lines in this and other single channel records indicate open and shut levels, as marked by "o" and "s." In the presence of blockers, open and shut levels are determined based on the current amplitude in control records. When channel closure is rare, occasional long shut segments are deliberately included in single channel records in order to show the shut levels.

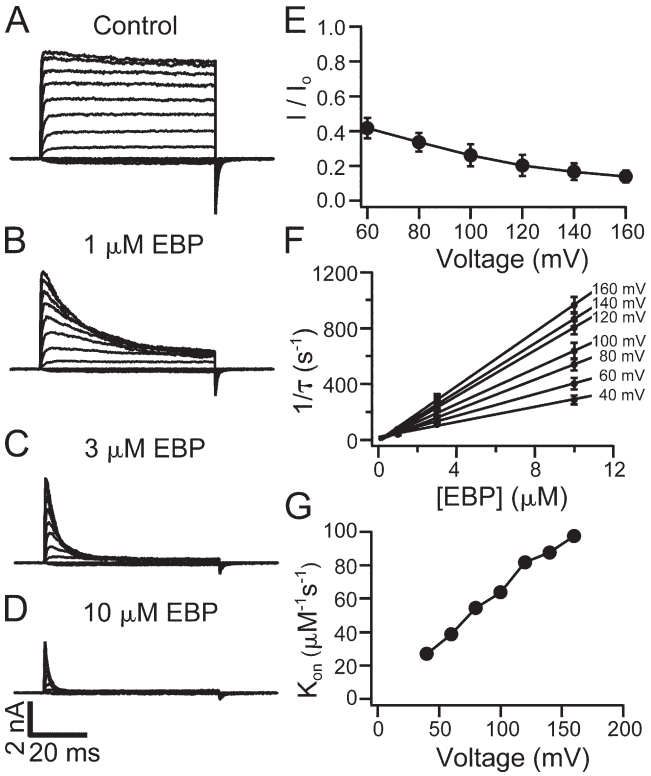

Figure 4. Voltage and concentration dependence in the block of BK channels by EBP. Macroscopic BK currents were recorded in response to depolarizations of membrane potential from −80 to 160 mV at 20-mV steps. Current families are shown in the absence (A) and presence of 1 μM EBP (B), 3 μM EBP (C), and 10 μM EBP (D). (E) Remaining fractions of currents in the presence of 1 μM EBP (compared with control) at the end of 60-ms pulses at positive potentials were measured from six patches, and the average and SEM are plotted as a function of membrane potential. Error bars representing SEM in this and other figures are often smaller than the symbols. Note in B that currents may not reach steady state within 60 ms at all potentials in the presence of 1 μM EBP. (F) EBP block is fitted with single exponential time course at positive potentials in the presence of 1, 3, and 10 μM EBP from six patches. The reciprocals of the time constant ($1/\tau$) are averaged and plotted as a function of EBP concentration with error bars representing SEM. The relations between $1/\tau$ and EBP concentration are fitted with straight lines at each potential. (G) K_{on} values measured by the slope of the fitted lines in F are plotted as a function of membrane potential. The solid lines connecting the data points in E and G have no physical meaning.

($1/\tau$) from such fits are plotted in Fig. 4 F ($n = 6$). At each membrane potential, $1/\tau$ seems linearly dependent on the concentration of EBP and can be well fitted by straight lines. Such an observation is consistent with a bimolecular block reaction, in which only one peptide molecule binds and blocks each BK channel. In fact, such bimolecular nature of the block was previously established for ShBP and its homologues in both BK and Shaker channels (Foster et al., 1992; Toro et al., 1992; Murrell-Lagnado and Aldrich, 1993b). With the assumption that the dissociation rate is not affected by EBP concentration, the slope of linear fits in Fig. 4 F should directly measure the association rate constant (K_{on}), because $1/\tau = [EBP] \times K_{on} + K_{off}$. As shown in Fig. 4 G, K_{on} measured in this way clearly depends on membrane potentials, with larger depolarizations resulting in higher association rate constants. Voltage dependence of the apparent K_{off} is not analyzed in the present study, although some dependence is expected based on earlier studies at single channel level (Foster et al., 1992; Toro et al., 1992, 1994).

Given that the voltage dependence can potentially account for the time dependence in EBP block of BK channels, we need to more rigorously establish the state dependence of the block in order to employ EBP to address the location of channel gates. First we ask whether the receptor site for EBP is inside the channel pore. Voltage dependence of the apparent association rate constant (Fig. 4 F) is consistent with the idea that positively charged EBP molecules penetrate into the BK channel pore, thus sensing a fraction of the potential drop across the membrane. The involvement of such long-range electrostatic interactions in enhancing diffusion of the peptide toward its binding site was well established for ShBP and homologues with Shaker channels in previous studies (Murrell-Lagnado and Aldrich, 1993a,b). However, a more direct way to establish a pore blocker has been through the competition with internal QA blockers (Choi et al., 1991). At the single channel level, it was previously shown that the short blocks of BK channels by ShBP were competitively relieved by the presence of a high concentration of TEA, while the competition between TEA and the long blocks was not exclusively analyzed (Foster et al., 1992; Toro et al., 1992). Our previous study shows that internal TBA results in fast block of BK channels at submillimolar concentrations. We therefore tried to determine whether TBA competes with EBP in blocking BK currents at positive potentials. As shown in Fig. 5, the addition of 500 μM TBA on top of 3 μM EBP reduces the peak current to about half and slows the time-dependent EBP block by about twofold when compared with 3 μM EBP alone. This result is as expected for a complete competition mechanism between TBA and EBP: OTBA↔O↔OEBP, in which TBA and EBP cannot bind to the channel simultaneously. At positive potentials, 500 μM TBA was known to inhibit ~50% of BK current at steady state (Li and Aldrich, 2004). Because TBA block reaches its equilibrium much faster compared with EBP block, it causes ~50% reduction in the peak current. Also because of the fast kinetics of TBA block, essentially only about half of the channels (that haven't already bound with EBP) are accessible to EBP at any given time; thus the effective rate of EBP block is halved. Although this competition does not necessarily mean that TBA and EBP share the same binding site, it does argue that binding of EBP occurs inside the BK channel pore near the QA binding site, such that their bindings are mutually exclusive.

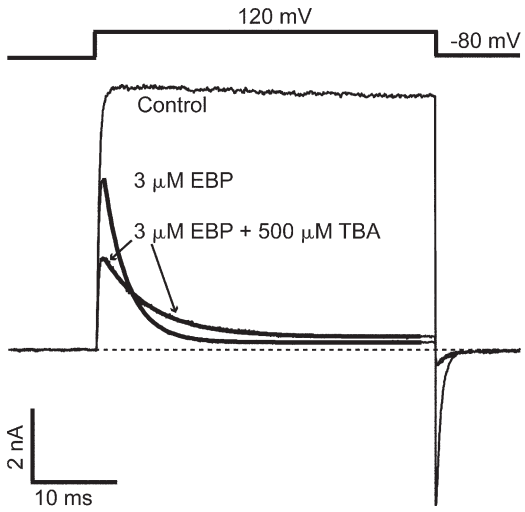

Figure 5. Apparent EBP block rate of BK channels is slowed by TBA. Macroscopic BK currents elicited by the shown voltage protocol were recorded without blockers (control), with 3 μM EBP, and with 500 μM TBA in addition to 3 μM EBP. Currents in the presence of 3 μM EBP are fitted with single exponential time course (thick smooth lines). Time constants used in the fitting are τ = 2.8 ms (3 μM EBP alone) and τ = 5.6 ms (3 μM EBP plus 500 μM TBA).

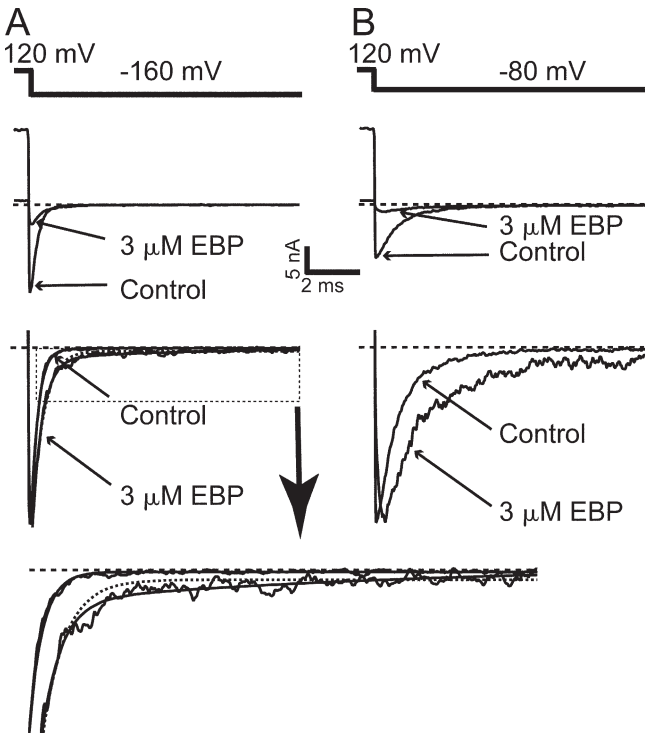

Figure 6. Deactivation of BK channels is slowed by EBP. (A) After a depolarization to 120 mV, tail currents were recorded at −160 mV in the absence (control) and presence of 3 μM EBP. Large currents were deliberately selected for better visualization of the tail currents. Pipette access resistance in bath in this experiment was 0.8 MΩ. Tail currents normalized to their peak amplitude are shown in the bottom panels. Normalized control tail current at −160 mV is fitted with a single exponential time course (smooth line) with τ = 0.25 ms, while normalized tail current in 3 μM EBP is fitted with double exponential time course (smooth line) with time constants of τ_{fast} = 0.37 ms and τ_{slow} = 7.3 ms. Dotted line is an attempt to fit the tail current in 3 μM EBP with a single exponential component (see the zoomed view of the traces inside the dotted box in the bottom panel). (B) Tail currents at −80 mV in the absence (control) and presence of 3 μM EBP. Note the "hook" in the normalized tail current in the presence of 3 μM EBP.

We then ask whether EBP acts as an open-channel blocker on BK channels, as has been established in the block of Shaker channels by synthesized ball peptides and the intact inactivation gate (Zagotta et al., 1990; Demo and Yellen, 1991). A key characteristic of open-channel blockers is that they typically slow down the deactivation by a "foot in the door" mechanism (Yeh and Armstrong, 1978), which means that these internal blockers, when bound to the channel, physically prevent the channel gate from being closed, even when a closed conformation is favored at hyperpolarized potentials. Such slowing of deactivation may not manifest when the blockers can be trapped inside the channel cavity, as previously proposed for the QA block of BK channels (Li and Aldrich, 2004). However, the enormous size of EBP makes it unlikely to be easily trapped inside the cavity, if its binding site is actually behind the channel gate. Indeed, in the presence of EBP, the deactivation of BK channels as shown by the tail current is slowed compared with the control trace (Fig. 6, A and B). Deactivation of control BK currents at negative potentials is fitted well with a single exponential time course (Cui et al., 1997; Li and Aldrich, 2004) (Fig. 6 A). Normalized tail current at −160 mV in the presence of 3 μM EBP is clearly slower compared with control, and its time course requires at least two exponential components to fit. This is consistent with the simple open-channel-block scheme: Closed↔Open↔Blocked. Two exponentials are clearly needed to fit tail currents in the presence of EBP at all negative potentials less than −80 mV. The time constant of the fast component decreases rapidly with membrane potential (from ∼2 ms at −60 mV to ∼0.3 ms at −160 mV) and the slower one remains relatively voltage insensitive (∼10 ms). At membrane potentials greater than −80 mV, the time constants of the two components become closer and the amplitudes of tail currents become smaller so that the necessity for a two-exponential fit is less clear. At each negative potential less than −80 mV, the time constants for the faster component of deactivation are similar to the time constants for the control tail currents at the same membrane potential, suggesting that this component reflects the unblocked channels at the time of repolarization undergoing normal deactivation, while block by EBP during deactivation is relatively too slow to have an effect on its time course. On the other hand, the slower component likely reflects the stably blocked

channels going through unblock then deactivation. Because of its much longer time constant than the fast component, the slow component has a much smaller relative amplitude. Modeling the tail currents with a C↔O↔B model to reproduce the time constant and relative amplitude of the slow component suggests that the off rate of EBP at negative potentials is rather voltage insensitive, at ~100 s^{-1}. Although we were not able to directly measure the off rate of EBP at negative potentials, such an estimate seems consistent when compared with the analysis of ShBP-blocked Shaker channel tail currents (Murrell-Lagnado and Aldrich, 1993a).

Interestingly, at around −80 mV, a "hook" in the tail current in the presence of EBP is visible (Fig. 6 B). The apparent rising phase of the hook suggests that the number of blocked channels unblocking is larger than the number of open channels closing in a unit of time. Considering the fast deactivation rate of BK channels at −80 mV, this suggests that a small fraction of blocked BK channels undergo very fast unblock at the beginning of hyperpolarization. Such fast unblock is not expected based on the slow dissociation rate of the EBP block, and suggests that EBP may produce multiple kinetically distinct block states in BK channels, with at least one unblocking very rapidly at negative potentials. At more hyperpolarized potentials such as −160 mV (Fig. 6 A), such a "hook" is less visible most likely because it is covered by the limited temporal resolution and faster deactivation process. However, by comparing the peak amplitude of the tail current at −160 mV in the presence of EBP with the control trace, it is obvious that immediately after repolarization, significantly less channels are blocked than in the preceding depolarization, again suggesting that a fraction of channels unblock very fast. Similar analysis in the block of Shaker channels by ShBP in a previous study also identified a component of the block that is very unstable at negative membrane potentials (Murrell-Lagnado and Aldrich, 1993a).

To directly address the state dependence of EBP block independently of membrane potential, we tried to vary the P_o and the activation kinetics of BK channels under the same potential. It has been established that lower internal Ca^{2+} concentration can decrease the P_o and slow down the activation kinetics of BK channels. We therefore compared the block of EBP under High Ca^{2+} and Low Ca^{2+} conditions. Fig.7 illustrates the effect of activation kinetics on the block by EBP. Consistent with earlier studies on BK channels, we found the activation kinetics to be much slower in Low Ca^{2+} internal solution than the High Ca^{2+} solution (compare the control traces in Fig. 7 A). It is obvious in Fig. 7 A that the block by EBP is also slowed in Low Ca^{2+} solution such that currents in the High and Low Ca^{2+} solution "cross over." This is not consistent with a state-independent block mechanism. Fig. 7 B shows simulated currents with such a mechanism, in which the amount of block is only dependent on voltage, regardless of whether channels are open or closed. Under the same potentials, all channels, closed or open, will become blocked at the same rate governed by the voltage according to this model. Therefore at any given time, there can't be more open and unblocked channels, therefore more currents, in the Low Ca^{2+} than the High Ca^{2+} condition. On the other hand, a state-dependent block mechanism, in which the channels need to first open to be blocked, predicts the results shown in Fig. 7 A. As shown in Fig. 7 C, a crossover between the currents in High and Low Ca^{2+} is predicted by such a model. This is because in this mechanism the slow activation limits the rate of block in

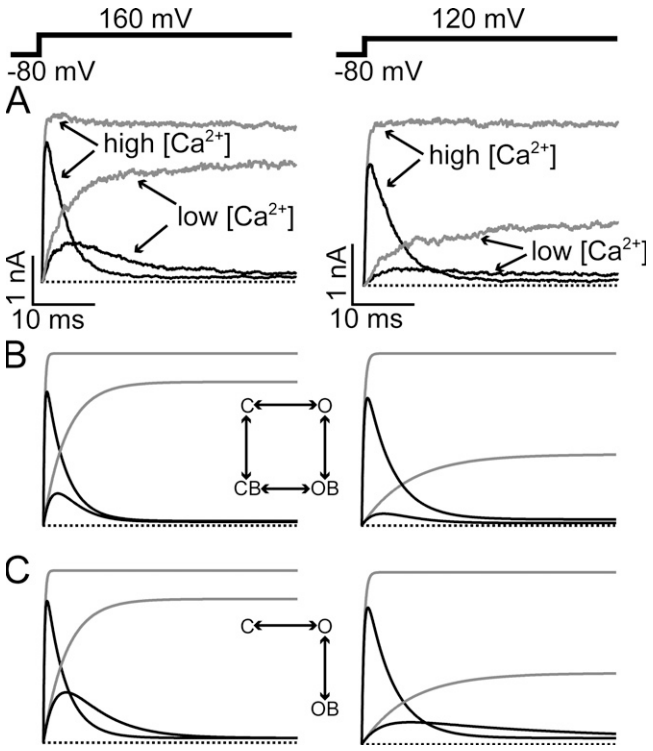

Figure 7. Dependence of EBP block on activation kinetics suggests state-dependent-block mechanism. (A) Macroscopic BK currents in the absence (gray traces) and presence (black traces) of 3 μM EBP were recorded at 160 and 120 mV in High and Low Ca^{2+} solutions. (B) Simulated currents at two different potentials using the completely state-independent-block model shown in the inset. Activation kinetic parameters in the modeling were obtained from single exponential fitting of the activation time course and averaged P_o at given membrane potentials in control currents in each Ca^{2+} concentration. The block rates were determined by the steady-state block level and single exponential fitting of the current decay in High Ca^{2+}, where the activation is much faster compared with the rate of block. The two horizontal transitions are assumed to have the same rates, so are the two vertical transitions. (C) Simulated currents using a classic open-channel-block model shown in the inset. All rates that are present in this model are the same as in B. All channels are assumed to be at the closed and unblocked state before depolarization in both B and C.

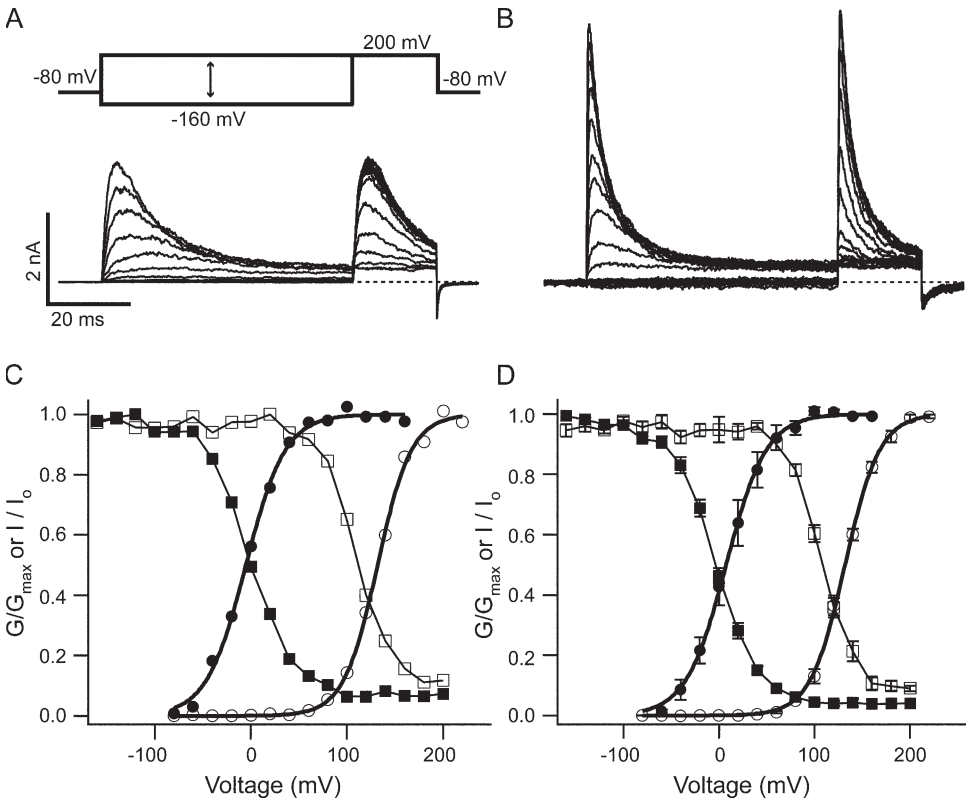

Figure 8. Block of BK channels by EBP is dependent on the open probability. Macroscopic BK currents in the presence of 3 μM EBP were recorded using the shown voltage protocol. From a holding potential at −80 mV, membrane potential was stepped to a value between −160 and 200 mV at 20-mV steps for 60 ms, followed by a 20-ms test pulse at 200 mV. Currents shown in A and B are from the same patch with different Ca^{2+} concentrations. Low Ca^{2+} solution was used in A and High Ca^{2+} in B. (C) From the same patch shown in A and B, the relative conductance of macroscopic BK channels as a function of membrane potential was determined in the absence of EBP by isochronal tail current amplitude at −80 mV with Low (open circles) or High Ca^{2+} solution (solid circles). Both sets of data were fitted with the Boltzmann function $G = G_{max}/(1 + \exp(-zF(V - V_{1/2})/RT))$ (smooth lines) and then normalized to the maximum of the fit. In this function, $V_{1/2}$ is the membrane potential at which half of the channels are open, and z is the apparent equivalent gating charge, while all other parameters have their normal meanings. Values used for the fitting are $V_{1/2} = 131.8$ mV, $z = 1.46$ (Low Ca^{2+}) and $V_{1/2} = -5.1$ mV, $z = 1.25$ (High Ca^{2+}). Relative peak current amplitudes (I/I_o, I_o is the maximal peak amplitude in the presence of EBP) during the test pulse in A and B are shown together with the P_o-V curves as functions of the prepulse membrane potential for Low Ca^{2+} (open squares) and High Ca^{2+} (solid squares). Lines connecting the squares have no physical meaning. (D) Same experiments described in A–C were repeated on three other patches. The average of the four patches is plotted with SEM. Values used to fit the P_o-V relations (smooth lines) are $V_{1/2} = 131.9$ mV, $z = 1.41$ (Low Ca^{2+}) and $V_{1/2} = 7.0$ mV, $z = 1.22$ (High Ca^{2+}).

Low Ca^{2+}. The activation process of BK channels is known to be more complicated than a single exponential process; therefore the models shown in Fig. 7 are oversimplified. However, it clearly demonstrates that the block of EBP is much more favored in an open configuration than a closed one.

Fig. 8 illustrates the effect of P_o on EBP block. In the absence of EBP, the Low Ca^{2+} internal solution shifts the P_o-V relation to the right by ∼130 mV (Fig. 8, C and D) relative to the High Ca^{2+} case, a value similar to those from earlier studies on BK channels (Cui et al., 1997; Li and Aldrich, 2004). Low Ca^{2+} therefore results in lower P_o at any given membrane potentials between −80 and 160 mV when compared with the High Ca^{2+} condition. As shown in the voltage protocol in Fig. 8 A, membrane potentials were held at different levels between −160 and +200 mV for 60 ms before a short test pulse at +200 mV. The test pulse was used to roughly estimate the fraction of channels that remained unblocked by the end of the 60-ms prepulse because the peak current amplitude during the test pulse is closely affected by how many channels remain unblocked right before the test pulse. The relative peak amplitudes during the test pulse were plotted as a function of the prepulse potential in Fig. 8 C together with the P_o-V relations. This procedure was repeated in three other patches, which yielded very similar results. The average of the four experiments is plotted in Fig. 8 D. The relative peak amplitudes are also affected by the kinetics of activation during the test pulse, as shown in Fig. 7 A. Therefore they don't directly measure the fractional block, although it is obvious that the more preblock, the smaller the peak current amplitude should be in the test pulse. Other complications are that at lower membrane potentials, multiple block states may exist, and that the block may not reach fully steady state by the end of the 60-ms prepulses. However, despite the aforementioned limitations, the fact that the relation between the relative peak amplitude and the prepulse potential was right shifted in the Low Ca^{2+} solution by a similar amount as the P_o-V relations strongly suggests that block of BK channels by EBP is closely dependent on the open probability. For example, at membrane potentials between −80 and 80 mV, in the High Ca^{2+}

solution as the P_o changes from ~0 to ~1, the relative amplitude of the test currents changes from ~1 to a steady level of <0.1, correlating with a change in the fraction of preblock from ~0 to >0.9. However, within the same membrane potential range in the case of Low Ca^{2+} concentration, where the P_o remains ~0, the relative amplitude of the test current doesn't change much. This is not expected if EBP block of BK channels is state independent, because in that case the same fraction of channels will be preblocked in both calcium concentrations, therefore the relative amplitudes of the test currents will be similarly affected within the same potential range. Instead, the close correlation between the relative amplitudes of test currents and P_o throughout a wide voltage range suggests that EBP block of BK channels is largely dependent on the open probability. Furthermore, such a close correlation in both calcium concentrations indicates that the block is directly affected by P_o but not calcium concentration per se.

In the following section, we look further into the properties of EBP block with the question of whether EBP binding site(s) in BK channels are similar to those in Shaker channels. Detailed analysis on block of Shaker channels by ShBP and its homologues have identified two most important features in peptide binding: charged residues within the C-terminal half of the peptide, which mainly influence the association rate by a long-range electrostatic mechanism; and hydrophobic residues in the N-terminal half of the peptide, which primarily affect the stability, thus the dissociation rate, of the peptide binding through hydrophobic interaction (Murrell-Lagnado and Aldrich, 1993a,b). Similar analysis on the block of single BK channels by ShBP and its homologues has concluded that the same two features are also critical for peptide binding (Toro et al., 1994). However, previous studies on the block of BK channels by ShBPs were focused mainly on the short block events, where the dissociation rate of ball peptides is significantly higher compared with ShBP block of other channel types. This discrepancy may suggest that the binding of ball peptide with channel is mechanistically different between BK and other channels. Finding in the current study that EBP primarily produces long block states in BK channels with dissociation rates comparable to those in other K^+ channels, we want to establish whether the binding of EBP to BK channel is also influenced by the two aforementioned mechanisms. Additionally, these two proposed mechanisms for peptide–channel interaction were inferred from the effects of peptide mutations, implying the involvement of local negative charges and hydrophobic residues near the binding site in the channel. Such implications have been supported by the effects of mutations in some voltage-dependent K^+ channels on the binding affinity of either the tethered inactivation gate or synthesized ball peptide (Isacoff et al., 1991; Zhou et al., 2001), but

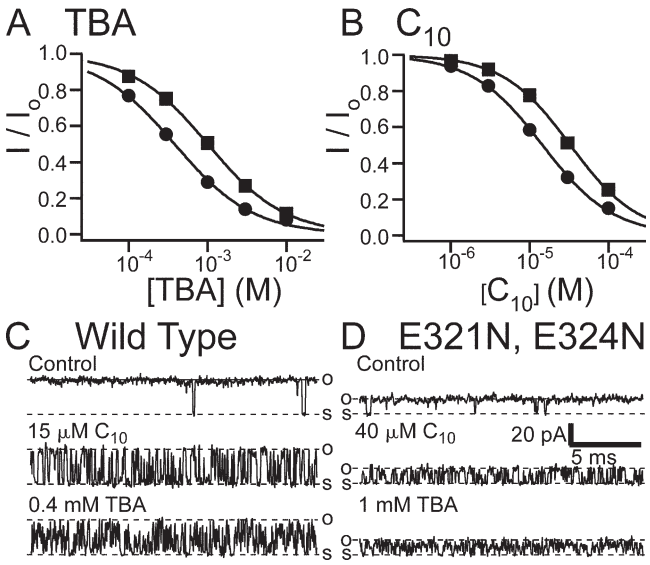

Figure 9. Affinities and association rates for QA blockers are reduced in the E321N, E324N mutant. (A) Dose–response curves for TBA block of the E321N, E324N mutant (solid squares) and wild-type BK channels (solid circles). Remaining fractions of steady-state currents at 120 mV in the presence of different concentrations of TBA were determined from five patches for wild type and nine patches for the mutant. The average values and SEM are plotted as functions of TBA concentration. Smooth lines are fitted curves with Hill equation: $I/I_o = 1/(1 + ([TBA]/K_d)^n)$. Values used in the fitting are K_d = 1.01 mM, n = 0.89 (mutant) and K_d = 0.38 mM, n = 0.87 (wild type). (B) Dose–response curves for C_{10} block of the E321N, E324N mutant (solid squares) and wild-type BK channels (solid circles). Remaining fractions of steady-state currents at 100 mV in the presence of different concentrations of C_{10} were determined from eight patches for the mutant and six patches for wild-type BK channels. The average values and SEM are plotted as functions of C_{10} concentration. Smooth lines are fitting curves of the data with Hill equation: $I/I_o = 1/(1 + ([C_{10}]/K_d)^n)$. Values used in the fitting are K_d = 32.8 μM, n = 1.01 (mutant) and K_d = 14.5 μM, n = 0.97 (wild type). (C) Single channel recordings of a wild-type BK channel at 120 mV in the absence (control) and presence of 15 μM C_{10} or 0.4 mM TBA. (D) Single channel recordings of an E321N, E324N channel at 120 mV in the absence (control) and presence of 40 μM C_{10} or 1 mM TBA.

similar experiments haven't been conducted in BK channels. Fortunately, we have some available BK channel mutants that allow us to test whether the electrostatic and hydrophobic interactions are indeed important for the binding of EBP with BK channels.

Previous studies on BK channels have identified two negatively charged glutamates (E321, E324) near the inner mouth of the channel pore as being important for the single channel conductance via an electrostatic mechanism (Brelidze et al., 2003; Nimigean et al., 2003). These negative charges apparently raise the local concentration of K^+ near the inner mouth, thus increasing the conductance. Double mutation (E321N, E324N) at these glutamates was shown to decrease the single channel conductance by about half. We reason

that electrostatic interaction between the BK channel and positively charged EBP, if any, should also be affected in this mutant. In light of the complicated charge distribution in EBP, we first tested the effect of the mutation on the block of BK channels by two QA molecules, TBA and C_{10}, which were discussed in our earlier study (Li and Aldrich, 2004). These two molecules, each with a net charge of +1, can largely be considered as having point charges. Our results with macroscopic currents show that the apparent affinity of block by both TBA and C_{10} was decreased by ~2.5-fold in the E321N, E324N mutant (Fig. 9, A and B). This difference can be explained by an electrostatic mechanism, in which negatively charged glutamates in wild-type BK channels increase the effective concentration of TBA or C_{10} by ~2.5-fold, a number similar to the factor of increase on effective K^+ concentration for conductance (Brelidze et al., 2003). Such a mechanism is supported by our single channel recordings, indicating that only the association rates of blockers are affected by the double mutation (Fig. 9, C and D). For example, the dissociation rates of C_{10} block at 120 mV, measured by the mean shut dwell time (by assuming all shut–open transitions as due to block and unblock), are similar between wild type and the E321N, E324N mutant (6.4 ± 0.5 ms^{-1} for wild type and 7.8 ± 0.6 ms^{-1} for mutant; mean ± SD, $n = 5$ for each). On the other hand, the difference in association rates between wild type and mutant channels can be largely compensated by an increase in C_{10} concentration for mutant by ~2.5-fold. (wild type: 9.0 ± 1.6 ms^{-1} in 15 μM C_{10} and mutant: 12.5 ± 1.1 ms^{-1} in 40 μM C_{10}; mean ± SD, $n = 5$ for each). The very fast dissociation rate of TBA block precluded direct kinetic measurements at the single channel level. However, increasing TBA concentration by 2.5-fold (1 mM) in mutant channels produces blockage of single channels that are qualitatively very similar when compared with wild-type channels in the presence of 0.4 mM TBA (Fig. 9, C and D). This is consistent with the idea that only the association rate of TBA is affected by the E321N, E324N mutation.

Considering the long-range electrostatic mechanism, any given change in the local potential should have a larger effect on the concentration of species with higher valence. Therefore a larger difference in the apparent affinity is expected for EBP, which has a net charge of +6. Indeed, EBP has a much reduced apparent affinity for the E321N, E324N double mutant channels when compared with wild type. As shown in Fig. 10 A, 100 μM of EBP blocks <60% of the currents, whereas in wild-type channels, 3 μM EBP results in nearly complete block (Fig. 2 A and Fig. 4 C). To quantify the differences, the steady-state block of wild-type BK channels by submicromolar concentrations of EBP was measured at 120 mV with long pulses (500 ms). The fitted dose responses in Fig. 10 B indicate that apparent affinity of EBP block decreases by more than two orders of magnitude in the double mutant. Another obvious difference between the block of the double mutant and wild-type channels is that the kinetics of block in mutant channels is mainly fast. Two exponential components are typically needed to fit the time-dependent current decay for the mutant. At around half block concentration at 120 mV, the dominating component has a time constant of a few milliseconds, typical of the short blocks by ShBP. A very small component has a time constant of hundreds of milliseconds, suggestive of the long blocks. This difference is also obvious at the single channel level. EBP produces primarily block events lasting hundreds of milliseconds at 80 mV in wild-type BK channels (Fig. 3 B); whereas in mutant channels, EBP results in mainly short block events lasting a few milliseconds (Fig. 10 C). The kinetic changes in the block of mutant channels indicate that the effect of mutation on EBP block cannot be explained by a simple decrease in association rate as the case for C_{10} and TBA, because the relative frequency of long and short block events was also changed. This will be discussed further in the next section. The effect of E321N, E324N mutation on block by native ShBP was only roughly estimated. 100 μM ShBP (highest concentration tested) blocks ~20% percent of the E321N, E324N currents at 120 mV (unpublished data) while it blocks ~70% of wild-type BK currents. This corresponds to a decrease in the apparent affinity by ~10-fold as a result of the double mutation. This lower number relative to the change in affinity for EBP appears reasonable for an electrostatic mechanism considering less net charge in native ShBP.

Results with another mutant of the BK channel suggest that hydrophobic interaction between peptide and channel is also important for the binding of EBP. Given the likelihood that the tethered inactivation gate and synthesized ball peptides may bind close to the QA binding site, which has been structurally shown to be deep into the channel cavity near the selectivity filter (Zhou et al., 2001), it is conceivable that the hydrophobic amino acids in the N terminus of the ball peptide interact with the hydrophobic residues lining the wall of channel cavity to stabilize the binding. Previous studies have shown that both the number and the location of hydrophobic residues in the peptide are important for the stability of binding between ball peptides and BK channels (Toro et al., 1994). However it is not known whether the residues lining the pore of BK channels are also important, as would be predicted by a hydrophobic interaction. To address this question, we have used a construct of the BK channel (S6/2-KcsA) made in our lab by K. Hogan in which the entire lower half of the S6 transmembrane helix lining the pore (L312-I326) is replaced with the corresponding sequence from KcsA channel. Single S6/2-KcsA channels demonstrate constitutive flickery openings at negative membrane potentials

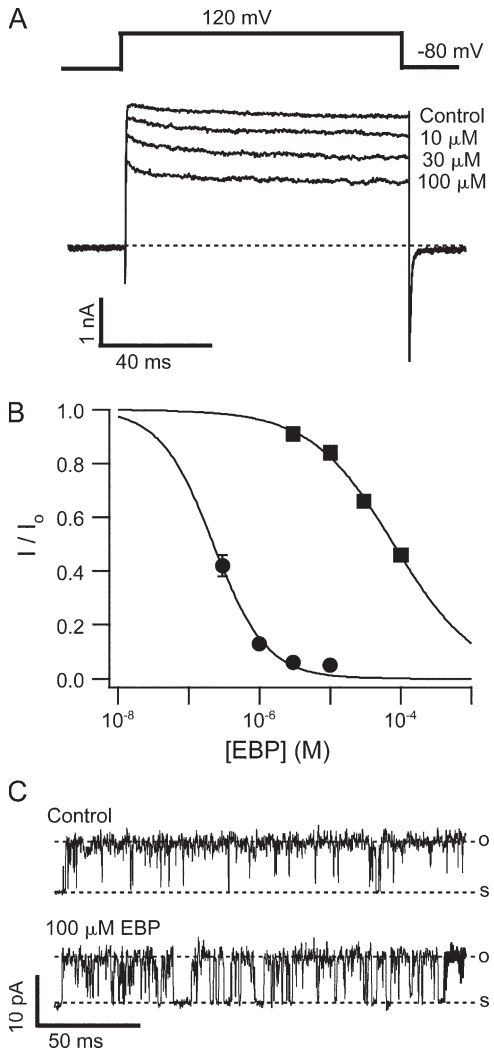

Figure 10. The E321N, E324N mutation affects both affinity and kinetics of EBP block. (A) Macroscopic currents were recorded from an inside-out patch expressing the E321N, E324N mutant channels at 120 mV in the absence (control) and presence of 10, 30, and 100 μM EBP. Currents were not leak subtracted by P/4 protocol due to significant openings even at very negative potentials. Instead, current recorded in the presence of 20 mM TBA from the same patch was subtracted from the traces to remove most of the leak and capacitance transient. TBA at this concentration blocks nearly 100% of mutant currents, as suggested in Fig. 9 A. (B) Dose–response curves for EBP block of the E321N, E324N mutant (solid squares) and wild-type BK channels (solid circles). Remaining fractions of steady-state currents at 120 mV in the presence of different concentrations of EBP were determined from 11 patches for mutant and 5 patches for wild-type BK channels. Very long pulses (500 ms) were used to determine the steady-state current levels when wild-type BK channels were treated with submicromolar concentration of EBP. The average values and SEM are plotted as functions of EBP concentration. Smooth lines are fitting curves of the data with Hill equation: $I/I_o = 1/(1 + ([EBP]/K_d)^n)$. Values used in the fitting are K_d = 89.0 μM, n = 0.72 (mutant) and K_d = 0.22 μM, n = 1.16 (wild type). (C) Single channel recordings of an E321N, E324N mutant channel at 80 mV in the absence (control) and presence of 100 μM EBP. Records were digitally filtered at 2 kHz.

(Fig. 11 C, trace a) regardless of internal Ca^{2+} concentrations, while at positive potentials they rarely close (Fig. 11 C, trace b and d). When macroscopically expressed, these channels conduct currents that almost look like leak currents, except that they are selective for K^+ (unpublished data) and sensitive to millimolar concentrations of TBA (Fig. 11 D). Indeed TBA has almost exactly the same affinity in the S6/2-KcsA construct as in wild-type BK channels (Fig. 11 A). By comparison to the E321N, E324N mutant, where the loss of negative charges reduces apparent affinity of TBA, this result is particularly surprising because in the S6/2-KcsA construct, these two negatively charged glutamates were changed into alanine and threonine, both uncharged. Additionally, the single channel conductance for the S6/2-KcsA channels is reduced similarly as for the E321N, E324N mutant compared with wild type. This finding suggests that the TBA binding site is unaffected by swapping the lower half of the S6 helix, and the loss of electrostatic contributions by E321 and E324 to TBA binding is compensated for by some unknown mechanisms. In a striking contrast to TBA, the apparent affinity of C_{10} is decreased by almost two orders of magnitude in the S6/2-KcsA construct (Fig. 11 B). As a result, C_{10} has a lower affinity than TBA for these channels. By comparison, in wild-type BK channels, the affinity of C_{10} is ~30 times higher than that of TBA. It has been established that long tail QA molecules such as C_{10} have increased affinities for K^+ channels mainly because the hydrophobic interaction between the tail and the channel wall stabilizes the binding, dramatically decreasing the dissociation rate (Choi et al., 1993). Comparing the structural features of C_{10} with TBA, our results suggest that the hydrophobic interaction between the tail of C_{10} and the channel wall is largely disrupted in the S6/2-KcsA construct, although the head group can still bind. If such is the case, the main mechanism for the decrease in C_{10} affinity in the S6/2-KcsA channels is expected to be a large increase in dissociation rate. This is indeed supported by our single channel recordings. At a concentration that blocks about half the macroscopic currents (1 mM), C_{10} induces block events in single S6/2-KcsA channels that are too fast to resolve in our recordings, indicating a very fast dissociation rate. As a result the apparent single channel conductance is reduced compared with control (Fig. 11 C, compare trace e with d). In contrast to the case of C_{10}, the block of single S6/2-KcsA channels by 0.4 mM TBA is kinetically very similar compared with that of wild-type BK channels (compare Fig. 11 C, trace c, with Fig. 9 C).

Although our results with C_{10} block don't provide specific information about which residues in the S6 transmembrane domain of BK channels are involved in the hydrophobic interaction with the tail of C_{10}, we reason that the hydrophobic interaction between the channel wall and ball peptides, if any, can be potentially affected

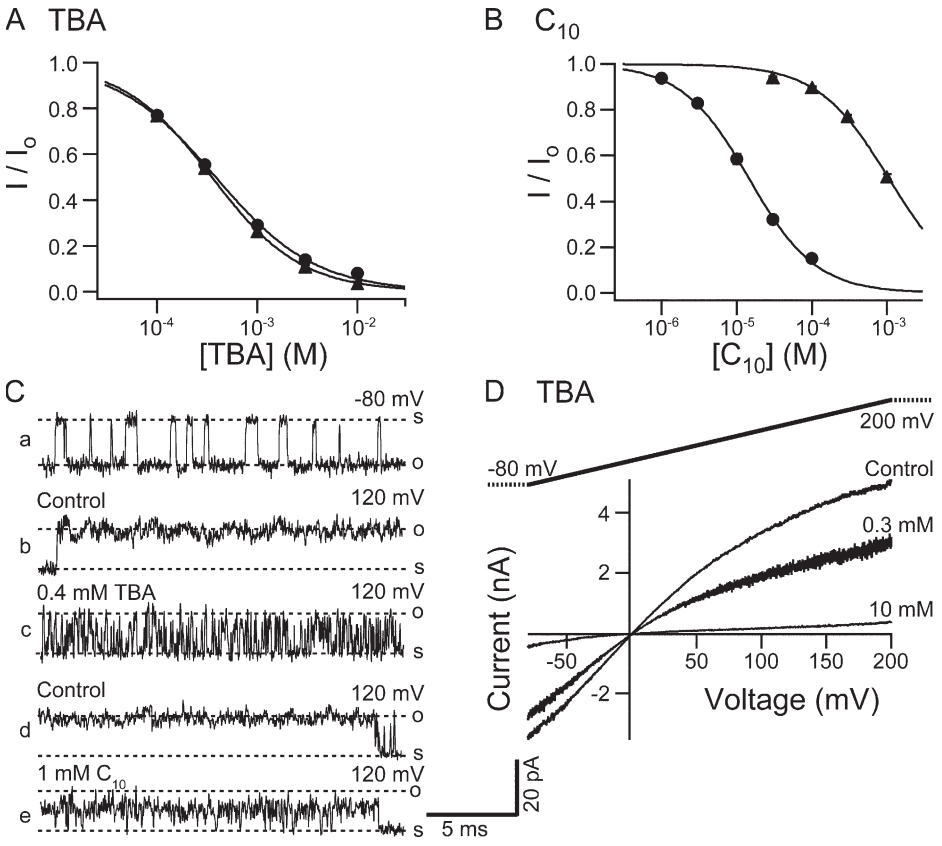

Figure 11. TBA and C_{10} affinities are differentially affected in the S6/2-KcsA mutant. (A) Dose–response curves for TBA block of the S6/2-KcsA mutant (solid triangles) and wild-type BK channels (solid circles). Remaining fractions of steady-state currents at 120 mV in the presence of different concentrations of TBA were determined from five patches for the S6/2-KcsA channels. Wild-type dose–response is the same as shown in Fig. 9 A. The average values and SEM are plotted as functions of TBA concentration. Smooth lines are fitting curves with Hill equation: $I/I_o = 1/(1 + ([TBA]/K_d)^n)$. Values used in the fitting are K_d = 0.35 mM, n = 0.97 (mutant) and K_d = 0.38 mM, n = 0.87 (wild type). (B) Dose–response curves for C_{10} block of the S6/2-KcsA mutant (solid triangles) and wild-type BK channels (solid circles). Remaining fractions of steady-state currents at 100 mV in the presence of different concentrations of C_{10} were determined from five patches for the S6/2-KcsA channels. Dose–response for wild-type BK channels is the same as shown in Fig. 9 B. The average values and SEM are plotted as functions of C_{10} concentration. Smooth lines are fitting curves of the data with Hill equation: $I/I_o = 1/(1 + ([C_{10}]/K_d)^n)$. Values used in the fitting are K_d = 1.06 mM, n = 0.95 (S6/2-KcsA) and K_d = 14.5 μM, n = 0.97 (wild type). (C) Single channel recordings of the S6/2-KcsA channels. a, b, and c are from one patch, d and e from another, at shown membrane potentials. (D) Macroscopic currents were recorded from an inside-out patch expressing the S6/2-KcsA mutant channels in response to a 200-ms voltage ramp from −80 to 200 mV. Shown traces are in the absence (control) and presence of 0.3 and 10 mM TBA. Currents are not leak subtracted.

similarly by the large scale mutation in the S6/2-KcsA channels. Indeed, 100 μM of EBP (highest concentration tested) results in the block of S6/2-KcsA current only by 23.0 ± 0.5% (mean ± SD, *n* = 5) at 120 mV (Fig. 12 A). This means that the apparent affinity of EBP for the S6/2-KcsA channels is more than three orders of magnitude lower than wild-type BK channels, and about threefold lower than EBP affinity in the E321N, E324N double mutant. Given the large-scale mutation in the S6/2-KcsA construct, it is difficult to rule out possible contribution by other mechanisms. Particularly because the block by TBA seems unaffected by this mutation, it is not clear how much the loss of negative charges at E321 and E324 contributes to the lower affinity for EBP. However, in light of the different responses to C_{10} versus TBA, it is likely that a disruption of the hydrophobic interaction between EBP and the wall of BK channel pore contributes significantly to the large decrease in binding affinity by destabilizing the binding between the channel and ball peptide. Consistent with this mechanism, block of single S6/2-KcsA channels by 100 μM EBP demonstrates very fast kinetics at 120 mV (Fig. 12 B). EBP fails to result in resolvable block events. Instead the single channel conductance is slightly decreased, which can potentially explain the ∼20% block of macroscopic currents at this concentration, although the rareness of closures and increased open-channel noise in this mutant make more quantitative analysis difficult. In contrast, 100 μM TBA (which also blocks ∼20% of macroscopic currents at 120 mV) results in flickery block events. This indicates that the dissociation rate of EBP in the S6/2-KcsA channels is even faster than that of TBA.

DISCUSSION

In the present study, we take advantage of the slow block of BK channels by a Shaker ball peptide homologue, EBP, to probe the inner pore of BK channels. Our results demonstrate that EBP behaves as a state-dependent blocker, in that peptide binding is much more favored in an opened BK channel. Furthermore, we find that the electrostatic and hydrophobic properties of the residues in S6 transmembrane helix of BK channels are

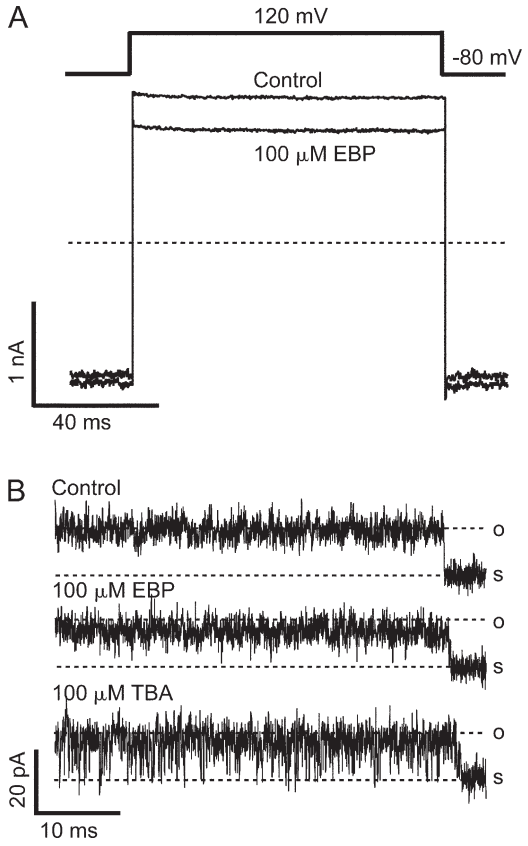

Figure 12. EBP block of the S6/2-KcsA channels demonstrates a reduced apparent affinity and an enhanced dissociation rate. (A) Macroscopic currents were recorded from an inside-out patch expressing the S6/2-KcsA mutant channels in response to a depolarization of membrane potential to 120 mV before (control) and after the application of 100 μM EBP. Currents were not leak subtracted by P/4 protocol because channels don't close even at very negative potentials. Instead, current recorded in the presence of 20 mM TBA from the same patch was subtracted from the traces to remove most of the leak and capacitance transient. TBA at this concentration blocks nearly 100% of mutant currents, as suggested in Fig. 11 (A and D). (B) Single channel recording of an S6/2-KcsA channel in the absence (control) and presence of 100 μM EBP or 100 μM TBA.

critical for the binding of ball peptides as well as QA ions. These data suggest that a conserved structural feature of the inner pore exists between BK and several other channel types.

The Cytoplasmic Gate

Early functional studies on voltage-dependent potassium (K_v) channels with QA ions (Armstrong and Hille, 1972) provided a hypothetical picture of K^+ channel, with the activation gate located at the cytoplasmic end of the pore. Recent structural studies on several types of K^+ channels (Doyle et al., 1998; Jiang et al., 2002a, 2003; Kuo et al., 2003; Long et al., 2005) and functional studies on Shaker K^+ channels (Holmgren et al., 1997; Liu et al., 1997; del Camino and Yellen, 2001; Hackos et al., 2002) have convincingly substantiated this hypothesis and proposed that the bundle crossing of the four S6 helices forms the gate in K_v channels. However whether such an activation gate is universally conserved across all channels, especially ligand-gated channels, remains to be determined. For example, accessibility studies on small conductance Ca^{2+}-activated K^+ channels (Bruening-Wright et al., 2002), ligand-sensitive inward rectifiers (Proks et al., 2003; Xiao et al., 2003), and CNG channels (Flynn and Zagotta, 2001) have suggested that their activation gates may be near or in the selectivity filter rather than at the cytoplasmic end of the S6 helices. In light of these findings, a question has been raised as to whether intracellular ligand-activated channels in general employ a different activation gate than voltage-activated channels (Bruening-Wright et al., 2002; Xiao et al., 2003). Additionally, studies on C-type inactivation of K^+ channels indeed demonstrate that part of the selectivity filter can function as a gate under certain circumstances (Lopez-Barneo et al., 1993; Yellen et al., 1994; Liu et al., 1996; Kiss et al., 1999). Accordingly, it has been proposed that K^+ channels may in fact have two activation gates that are energetically or mechanistically coupled with each other, one at the cytoplasmic end, the other at the selectivity filter (Korn and Trapani, 2005). BK channels are unique in that they are activated by both voltage and ligand (calcium). However, for BK channels, evidence either for or against a cytoplasmic gate has been rather surprisingly scarce. Accessibility study with engineered cysteines that has been successful in other ligand-gated channel types would be complicated by the presence of a large number of native intracellular cysteines in BK channels, and the possibility that BK channels can trap the modifying reagents (Phillips et al., 2003). In our earlier study on the block of BK channels by internal QA ions (Li and Aldrich, 2004), we showed that there is no apparent time dependence in the block, and that the presence of a blocker in the channel does not hinder the closure of the channel gate. Our tentative interpretation of the findings was based on the very fast QA block kinetics allowed for by a larger inner pore size, and a bigger cavity that can easily trap QA ions inside when the gate closes. However the extremely fast kinetics of QA block prevented us from ruling out an alternative interpretation, in which the channel gate is closer to the selectivity filter than the QA binding site is. In that case, the fast on and off rates of QA block and the lack of the "foot in the door" effect can both be easily explained. Indeed, there has been no clear evidence that the cytoplasmic ends of the S6 helices in BK channels move at all upon channel gating.

In this study, the slow block of BK channels by large ball peptides affords us a valuable opportunity to address the possibility of a cytoplasmic gate. Multiple lines of evidence suggest that EBP behaves as a pore blocker for BK channels. Effects of long-range electrostatic interactions on the association rate suggest that EBP penetrates

into the pore for binding, sensing part of the potential across the membrane; binding of EBP is mutually exclusive with that of TBA, a well-established pore blocker; mutations near or in the channel pore have dramatic effects on the apparent affinity. Therefore we feel it is appropriate to use EBP to probe the interaction between the pore blocker binding and gating conformational changes.

We have established that EBP acts on BK channels in the open-channel-block mechanism. EBP block of BK currents differs in several aspects from the block by QA ions in the previous study. First, EBP results in time-dependent block while leaving the onset of activation unaffected, suggesting that channels can only be blocked after they are open; and second, the presence of EBP induces a slow component in the process of deactivation, indicating that the closure of the channel gate is hindered by bound EBP. Lastly, we show that the rate and level of EBP block are dependent on the activation kinetics and open probability of BK channels.

Together these findings indicate that the binding site(s) of EBP is likely not accessible when the channel is closed, and that a significant widening at the cytoplasmic end of the inner pore results upon channel opening so that EBP can enter the pore. Such a conformational change is consistent with the proposed gating motion of S6 helices based on the structures of KcsA and MthK channels (Doyle et al., 1998; Jiang et al., 2002a) and functional studies on Shaker channels (Liu et al., 1997; del Camino et al., 2000; Webster et al., 2004). This suggests a channel gate intracellular to the blocker binding site(s), probably at the cytoplasmic end of S6 helices as previously suggested (Liu et al., 1997; Doyle et al., 1998; del Camino and Yellen, 2001; Jiang et al., 2002a). However, is this apparent gate for EBP indeed the sole activation gate in BK channel that is also responsible for controlling the permeation of K^+? Considering the large size of EBP (20 amino acids) in comparison with K^+ ions, it is possible that this gate only presents an effective barrier for large molecules such as EBP, while the actual obstruction of K^+ upon channel closure occurs somewhere else in the pore, e.g., near the selectivity filter, as the actual activation gate for K^+. In fact, studies on several ligand-gated channels have suggested that a conformational change also occurs at the cytoplasmic end of the pore upon gating, which can control the accessibility of larger molecules but not small ones (Flynn and Zagotta, 2001; Bruening-Wright et al., 2002; Xiao et al., 2003). Furthermore, results from a recent study in our lab suggest that the access of a smaller blocker of BK channels, bbTBA, may not be restricted by a cytoplasmic gate (Wilkens and Aldrich, 2006).

However, even if the "EBP gate" is not the actual activation gate for K^+ in BK channels, it most likely has significant functional importance. Previously it was shown that the size of the inner pore opening is a determining factor for the conductance of BK channels (Brelidze and Magleby, 2005); therefore the opening of the "EBP gate" upon gating is likely necessary for achieving the uniquely large conductance of BK channels. Considering that ball peptides can go through the inner pore of an opened K^+ channel with smaller conductance (such as Shaker), it is reasonable that the "EBP gate" in BK channels, when closed to EBP, will place a spatial limitation on the channel conductance. Additionally, if there is an activation gate other than the "EBP gate" that obstructs K^+, they are perhaps closely coupled to each other for the following reasons. (a) The "foot in the door" effect of EBP on the tail currents suggests that a bound EBP also prevents the other activation gate from being closed at deactivation. (b) A conformational change of the "EBP gate" independent of the actual activation gate for K^+ would likely result in a difference in the single channel conductance (e.g., a subconductance level) (Zheng and Sigworth, 1998), which is only occasionally seen in the single channel recordings of BK channels. Interestingly, if slight asynchrony between the two gates does occur during gating, it can potentially explain the brief lifetime subconductance states visited during the opening and closing transitions of some natively expressed BK channels (Ferguson et al., 1993).

Multiple Block States by Ball Peptides

Based on mutational and structural studies, the mechanism for the action of the intact N-type inactivation gate on K^+ channels has been proposed as the following: the N-terminal gate snakes into the pore as an extended peptide to bind in the hydrophobic central cavity, near the QA binding site (Zhou et al., 2001). It seems reasonable to think that the synthesized ball peptides should be able to bind to the same site. However, because the synthesized ball peptides in solution obviously have much more freedom than the tethered inactivation gate, it is possible that they can bind to the channel in more than one way. Previous studies on the block of BK channels by ShBP homologues revealed two kinetically distinct block states with different dwell times (Foster et al., 1992; Toro et al., 1992, 1994). For Shaker channels, two kinetically distinct components in the recovery from block also suggested that multiple block states exist (Murrell-Lagnado and Aldrich, 1993a).

Short block events (with lifetime of a few milliseconds) were previously found to dominate the block of single BK channels by ShBP (Foster et al., 1992; Toro et al., 1992, 1994), while the long block events (with life time of hundreds of milliseconds) are rare. This was confirmed by our macroscopic measurements with ShBP. In contrast, EBP block at positive potentials manifests mainly a slow single exponential decay in macroscopic BK currents and dwell times of hundreds of milliseconds at the single channel level (Figs. 2 and 3),

which suggests predominantly a block state with long lifetime. How do we explain the differences between ShBP and EBP? One possibility is that EBP binds BK channels in a totally different way than ShBP. Considering that the main differences between ShBP and EBP are charges, it is possible that some salt bridges form between the positively charged residues in EBP and the negatively charged residues in the channel, which stabilize the binding and produce a long lasting block state. This hypothesis is consistent with the previous identification of negatively charged residues in Shaker channel that are important for peptide binding (Isacoff et al., 1991), and supported by our finding that the loss of the negatively charged glutamates dramatically reduces apparent affinity and block dwell time. Previous studies on both Shaker and BK channels have concluded that the primary effects of net charges on binding affinity of ball peptides can be explained by changes in association rate, while the formation of salt bridges is unlikely (Murrell-Lagnado and Aldrich, 1993b; Toro et al., 1994). Particularly, even EBP results in predominantly short block events in BK channels at ~0 mV, while the long block events also exist in ShBP block of BK channels, although with a rather low frequency (Foster et al., 1992; Toro et al., 1992, 1994), suggesting that the extra positive charges in EBP are neither sufficient nor absolutely necessary for the long block states. However, we can't completely rule out the possibility that EBP at positive membrane potentials results in a unique long block state in wild-type BK channels that involves the formation of salt bridges, differing from the short and rare long block states near 0 mV and the block states in Shaker channels. If this is true, the different effects of EBP on E321N, E324N mutants and wild-type channels can be explained by proposing that E321 and E324 are directly involved in the formation of such salt bridges.

Alternatively, we can reconcile all the previous findings and our present results while keeping in line with the conclusion that net charges in the peptide primarily affect association rates. We propose the following explanation: EBP and native ShBP can both bind to BK channels in the same two states, resulting in short and long blocks respectively, but EBP at positive potentials has a much higher probability to bind in the long block state. Higher net positive charges, more depolarized membrane potentials, and negative charges in the channel near the inner mouth may collectively enhance specifically the association rate for the long block state (more than the association rate for the short block state) through a long-range electrostatic mechanism. This can explain why in cases of ShBP, EBP at 0 mV, or EBP on the E321N, E324N mutant, the short block events dominate. Since the long block state has a higher affinity, a decrease in the association rate for this state can explain the large decrease in EBP affinity of the E321N, E324N mutant. This mechanism requires that the association rates for short and long block states are differentially affected by electrostatic interactions but doesn't require the involvement of any salt bridges. In this mechanism, the short and long block states by EBP have the same physical nature as those by ShBP, although their relative frequencies are different. Additionally, this means that EBP can still bind E321N, E324N mutant at the same long block state as in wild-type channels, although with a much reduced frequency.

Although we have generally referred to the different states as the short and long block states, the existence of more than two individual states is not only possible but likely, based on earlier single channel studies (Foster et al., 1992; Toro et al., 1992, 1994) and our kinetic analysis of macroscopic BK currents in response to ShBP and EBP. The molecular nature for the different block states is not clear. It is unlikely due to impurity or instability of blockers because the relative frequency of different block states was not dependent on the batch and age of ball peptides. Additionally, multiple block states by ball peptides were also identified in several previous independent single channel studies in BK channels (Foster et al., 1992; Toro et al., 1992, 1994) and macroscopic studies in Shaker channels (Murrell-Lagnado and Aldrich, 1993a,b), where distinct block states were difficult to explain simply by low levels of contaminating peptides. Instead, the multiple block states could be a result of ball peptides binding to multiple physically distinct binding sites, or could be ball peptides assuming different conformations binding to the same site. The different block states could be sequential events after the initial binding of a ball peptide or they could be mutually exclusive processes. The present study does not provide enough information to resolve this question, but it suggests that long-range electrostatic mechanism can potentially differentially affect the association rates for different block states in BK channels.

Conserved Peptide Binding Mechanisms in BK Channels

In contrast to Shaker and several other spontaneously inactivating K^+ channels, most BK channels conduct sustained macroscopic currents without apparent time-dependent inactivation. No part of the pore-forming BK α subunit is suggestive of the presence of a tethered inactivation mechanism, although the N terminus of an auxiliary subunit, namely the β2 subunit, was found to result in the inactivation of BK channels in certain tissues (Wallner et al., 1999; Xia et al., 1999). However, the mechanism of β2 inactivation seems to differ significantly from that of Shaker inactivation (Solaro et al., 1997; Xia et al., 2003). Most importantly, the inactivation domain of β2 does not behave like a simple open-channel blocker. Additionally, other than the initial segment consisting of three critical residues, the specific structure and distribution of charges in the β2 inactivation domain are not required for the inactivation,

while such features are clearly important for the Shaker N-type inactivation gate. It is thus interesting to know whether the block of BK channels by ShBP homologues uses the same mechanism as their block of Shaker channels, or whether the binding sites for ball peptides are conserved between the two. Previously, mutational analysis was performed to identify structural features of Shaker ball peptides that are important for binding to BK channels (Toro et al., 1994). Based on the data with the short block of BK channels by ShBP homologues, it was found that a long-range electrostatic mechanism involving the charged amino acids is important for the association rate, while hydrophobic interactions between the peptide and the binding sites largely determine the dissociation rate. The same structural determinants were also found to modulate peptide binding to Shaker channels (Murrell-Lagnado and Aldrich, 1993a,b). These findings suggest that at least for the short block of BK channels, the mechanism of peptide binding is similar with Shaker channels. However, the large difference in the dissociation rate of native ShBP between Shaker and BK channels raises some doubt in their actual similarity. Due to their low incidence, the long blocks, which in fact appear more similar (in terms of dissociation rate) to the block of Shaker channels by ShBP homologues, were not analyzed in details in previous studies.

EBP at positive potentials produces predominantly long blocks, providing an opportunity to determine the important features that affect the long block state. Instead of modifying the structure of ball peptides, as has been conducted thoroughly, we investigated the effects of mutations in the BK channel. Since the electrostatic and hydrophobic interactions are mutual between the channel and the peptide, we argue that if these two types of interactions are indeed important for EBP binding, changes on the channel that disrupt such interactions should also affect the affinity. Indeed we find that the double mutation at E321N, E324N dramatically decreases the affinity of EBP in BK channels. These two negatively charged glutamates were previously identified as enhancing single channel conductance by raising the local concentration of K^+ through an electrostatic mechanism (Brelidze et al., 2003; Nimigean et al., 2003). We confirmed the electrostatic nature in the effect of the double mutation by measuring the change of affinities for two positively charged QA blockers, TBA and C_{10}. As discussed earlier, we propose that the decrease in apparent affinity of EBP in the E321N, E324N mutant can also be explained by a specific decrease in the association rate for the long block states.

Another BK channel mutant (S6/2-KcsA) seems to disrupt the hydrophobic interaction between the blocker and part of the channel wall. This mutation results in an even larger decrease in the affinity of EBP for BK channels. The lower half of the S6 helix of BK channel in this construct was replaced with KcsA sequence (L_{312}AMFASYVPEIIELI$_{326}$→I_{312}TSFGLVTAALATWF$_{326}$). It is obviously difficult to establish the specific mechanism to explain the change in EBP affinity because of the large scale of the mutation. However, we have reasons to think that disruption of hydrophobic interaction might play an important role. Our reasoning is based on the fact that the block by TBA and C_{10} are very differently affected in this construct (Fig. 11). Given the previous findings about the mechanism for QA binding in K^+ channels (Choi et al., 1993), it seems reasonable to think that the binding of TBA occurs above the swapped region, thus is left intact in the mutant. On the other hand, the hydrophobic interaction between the tail of C_{10} and the lower half of the S6 helices is likely disrupted in the mutant, resulting in a much reduced C_{10} affinity. In support of this, our single channel recordings clearly demonstrate that the dissociation rate of C_{10} is dramatically increased in the S6/2-KcsA channels, reflecting destabilization of binding. If such an interpretation is correct, then it is likely that the disruption of hydrophobic interaction between the channel and EBP also contributes to lowering the binding affinity in the S6/2-KcsA channels by destabilizing the binding. Again, our single channel recordings suggest that the dissociation rate of EBP is extremely fast in the S6/2-KcsA channels. The mechanism for the disruption of hydrophobic interaction in the S6/2-KcsA channels is completely unknown, and a simple comparison of the swapped sequences between BK and KcsA does not provide an obvious answer. Mutational studies on A-type K^+ channels demonstrated that five out of the six residues supposedly exposed to the cavity are important for the binding of inactivation gate (Zhou et al., 2001). Presumably both the number and position of some hydrophobic amino acids in the central cavity of BK channels are important for such an interaction, but the key residues remain to be determined. Interestingly, the hydrophobic interaction with C_{10} and EBP are similarly affected in the mutant, suggesting a common mechanism for binding.

Native ShBP produces only long block events in most other K^+ channels but mainly short block events in BK channels. Interestingly, increasing either net charge (in the current study) or hydrophobicity (Toro et al., 1994) of peptide can produce long block events in BK channels. It is tempting to propose that the binding of native ShBP is well stabilized by hydrophobic interaction in other K^+ channels, while in BK channels, ShBP is prone to bind at a less stabilized state where hydrophobic interaction is suboptimal. Increasing hydrophobicity in the peptide would help stabilize this state by providing stronger hydrophobic interaction, while increasing net charge would shift the binding to another state, which is more stabilized by optimized hydrophobic interaction.

ShBPs block various K^+ channel types and CNG channels (Kramer et al., 1994), among which many don't adopt the N-type inactivation of Shaker channels. However, all the studies, including ours, demonstrate that similar types of interaction are important for the peptide–channel binding, suggesting a conserved organization of the inner pore among these channels in terms of the peptide binding site(s), that is, binding site(s) surrounded by some negatively charged and some hydrophobic residues. Our findings suggest that these residues are also employed in the binding of QA ions to K^+ channels. It is unclear whether this is simply an evolutionary artifact due to the fact that these channels share the same precursor, or whether such a mechanism may serve some different functions in the noninactivating channels.

The authors thank Dr. Clay Armstrong for the kind gift of C_{10} and Dr. Christopher Miller for the E321N, E324N construct of BK channels. We thank Dr. Kate Hogan for generating the S6/2-KcsA construct of BK channels. We thank Dr. Jon Sack, Dr. Christina Wilkens, and Dr. Thomas Middendorf for insightful discussion about this project.

This work is supported by a grant from the Mathers Foundation.

Olaf S. Andersen served as editor.

Submitted: 16 February 2006
Accepted: 28 August 2006

REFERENCES

Armstrong, C.M., and B. Hille. 1972. The inner quaternary ammonium ion receptor in potassium channels of the node of Ranvier. *J. Gen. Physiol.* 59:388–400.

Bers, D.M. 1982. A simple method for the accurate determination of free [Ca] in Ca-EGTA solutions. *Am. J. Physiol.* 242: C404–C408.

Brelidze, T.I., and K.L. Magleby. 2005. Probing the geometry of the inner vestibule of BK channels with sugars. *J. Gen. Physiol.* 126:105–121.

Brelidze, T.I., X. Niu, and K.L. Magleby. 2003. A ring of eight conserved negatively charged amino acids doubles the conductance of BK channels and prevents inward rectification. *Proc. Natl. Acad. Sci. USA.* 100:9017–9022.

Bruening-Wright, A., M.A. Schumacher, J.P. Adelman, and J. Maylie. 2002. Localization of the activation gate for small conductance Ca^{2+}-activated K^+ channels. *J. Neurosci.* 22:6499–6506.

Butler, A., S. Tsunoda, D.P. McCobb, A. Wei, and L. Salkoff. 1993. *mSlo*, a complex mouse gene encoding "maxi" calcium-activated potassium channels. *Science.* 261:221–224.

Choi, K.L., R.W. Aldrich, and G. Yellen. 1991. Tetraethylammonium blockade distinguishes two inactivation mechanisms in voltage-activated K^+ channels. *Proc. Natl. Acad. Sci. USA.* 88:5092–5095.

Choi, K.L., C. Mossman, J. Aube, and G. Yellen. 1993. The internal quaternary ammonium receptor site of Shaker potassium channels. *Neuron.* 10:533–541.

Clay, J.R. 1995. Quaternary ammonium ion blockade of IK in nerve axons revisited. Open channel block vs. state independent block. *J. Membr. Biol.* 147:23–34.

Cox, D.H., J. Cui, and R.W. Aldrich. 1997. Separation of gating properties from permeation and block in *mslo* large conductance Ca-activated K^+ channels. *J. Gen. Physiol.* 109:633–646.

Cui, J., D.H. Cox, and R.W. Aldrich. 1997. Intrinsic voltage dependence and Ca^{2+} regulation of *mslo* large conductance Ca-activated K^+ channels. *J. Gen. Physiol.* 109:647–673.

del Camino, D., M. Holmgren, Y. Liu, and G. Yellen. 2000. Blocker protection in the pore of a voltage-gated K^+ channel and its structural implications. *Nature.* 403:321–325.

del Camino, D., and G. Yellen. 2001. Tight steric closure at the intracellular activation gate of a voltage-gated K^+ channel. *Neuron.* 32:649–656.

Demo, S.D., and G. Yellen. 1991. The inactivation gate of the Shaker K^+ channel behaves like an open-channel blocker. *Neuron.* 7:743–753.

Diaz, F., M. Wallner, E. Stefani, L. Toro, and R. Latorre. 1996. Interaction of internal Ba^{2+} with a cloned Ca^{2+}-dependent K^+ (*hslo*) channel from smooth muscle. *J. Gen. Physiol.* 107:399–407.

Ding, S., and R. Horn. 2002. Tail end of the s6 segment: role in permeation in shaker potassium channels. *J. Gen. Physiol.* 120:87–97.

Ding, S., and R. Horn. 2003. Effect of S6 tail mutations on charge movement in Shaker potassium channels. *Biophys. J.* 84:295–305.

Doyle, D.A., J. Morais Cabral, R.A. Pfuetzner, A. Kuo, J.M. Gulbis, S.L. Cohen, B.T. Chait, and R. MacKinnon. 1998. The structure of the potassium channel: molecular basis of K^+ conduction and selectivity. *Science.* 280:69–77.

Ferguson, W.B., O.B. McManus, and K.L. Magleby. 1993. Opening and closing transitions for BK channels often occur in two steps via sojourns through a brief lifetime subconductance state. *Biophys. J.* 65:702–714.

Flynn, G.E., and W.N. Zagotta. 2001. Conformational changes in S6 coupled to the opening of cyclic nucleotide-gated channels. *Neuron.* 30:689–698.

Foster, C.D., S. Chung, W.N. Zagotta, R.W. Aldrich, and I.B. Levitan. 1992. A peptide derived from the Shaker B K^+ channel produces short and long blocks of reconstituted Ca^{2+}-dependent K^+ channels. *Neuron.* 9:229–236.

Hackos, D.H., T.H. Chang, and K.J. Swartz. 2002. Scanning the intracellular S6 activation gate in the shaker K^+ channel. *J. Gen. Physiol.* 119:521–532.

Hamill, O.P., A. Marty, E. Neher, B. Sakmann, and F.J. Sigworth. 1981. Improved patch-clamp techniques for high-resolution current recording from cells and cell-free membrane patches. *Pflugers Arch.* 391:85–100.

Holmgren, M., P.L. Smith, and G. Yellen. 1997. Trapping of organic blockers by closing of voltage-dependent K^+ channels: evidence for a trap door mechanism of activation gating. *J. Gen. Physiol.* 109:527–535.

Horrigan, F.T., J. Cui, and R.W. Aldrich. 1999. Allosteric voltage gating of potassium channels I. *Mslo* ionic currents in the absence of Ca^{2+}. *J. Gen. Physiol.* 114:277–304.

Isacoff, E.Y., Y.N. Jan, and L.Y. Jan. 1991. Putative receptor for the cytoplasmic inactivation gate in the Shaker K^+ channel. *Nature.* 353:86–90.

Jiang, Y., A. Lee, J. Chen, M. Cadene, B.T. Chait, and R. MacKinnon. 2002a. Crystal structure and mechanism of a calcium-gated potassium channel. *Nature.* 417:515–522.

Jiang, Y., A. Lee, J. Chen, M. Cadene, B.T. Chait, and R. MacKinnon. 2002b. The open pore conformation of potassium channels. *Nature.* 417:523–526.

Jiang, Y., A. Lee, J. Chen, V. Ruta, M. Cadene, B.T. Chait, and R. MacKinnon. 2003. X-ray structure of a voltage-dependent K^+ channel. *Nature.* 423:33–41.

Kiss, L., J. LoTurco, and S.J. Korn. 1999. Contribution of the selectivity filter to inactivation in potassium channels. *Biophys. J.* 76:253–263.

Korn, S.J., and J.G. Trapani. 2005. Potassium channels. *IEEE Trans Nanobioscience.* 4:21–33.

Kramer, R.H., E. Goulding, and S.A. Siegelbaum. 1994. Potassium channel inactivation peptide blocks cyclic nucleotide-gated channels by binding to the conserved pore domain. *Neuron.* 12:655–662.

Kuo, A., J.M. Gulbis, J.F. Antcliff, T. Rahman, E.D. Lowe, J. Zimmer, J. Cuthbertson, F.M. Ashcroft, T. Ezaki, and D.A. Doyle. 2003. Crystal structure of the potassium channel KirBac1.1 in the closed state. *Science.* 300:1922–1926.

Li, W., and R.W. Aldrich. 2004. Unique inner pore properties of BK channels revealed by quaternary ammonium block. *J. Gen. Physiol.* 124:43–57.

Liu, Y., M. Holmgren, M.E. Jurman, and G. Yellen. 1997. Gated access to the pore of a voltage-dependent K^+ channel. *Neuron.* 19:175–184.

Liu, Y., M.E. Jurman, and G. Yellen. 1996. Dynamic rearrangement of the outer mouth of a K^+ channel during gating. *Neuron.* 16:859–867.

Long, S.B., E.B. Campbell, and R. Mackinnon. 2005. Crystal structure of a mammalian voltage-dependent Shaker family K^+ channel. *Science.* 309:897–903.

Lopez-Barneo, J., T. Hoshi, S.H. Heinemann, and R.W. Aldrich. 1993. Effects of external cations and mutations in the pore region on C-type inactivation of Shaker potassium channels. *Receptors Channels.* 1:61–71.

Murrell-Lagnado, R.D., and R.W. Aldrich. 1993a. Energetics of Shaker K channels block by inactivation peptides. *J. Gen. Physiol.* 102:977–1003.

Murrell-Lagnado, R.D., and R.W. Aldrich. 1993b. Interactions of amino terminal domains of Shaker K channels with a pore blocking site studied with synthetic peptides. *J. Gen. Physiol.* 102:949–975.

Neyton, J. 1996. A Ba^{2+} chelator suppresses long shut events in fully activated high-conductance Ca^{2+}-dependent K^+ channels. *Biophys. J.* 71:220–226.

Nimigean, C.M., J.S. Chappie, and C. Miller. 2003. Electrostatic tuning of ion conductance in potassium channels. *Biochemistry.* 42:9263–9268.

Phillips, L.R., D. Enkvetchakul, and C.G. Nichols. 2003. Gating dependence of inner pore access in inward rectifier K^+ channels. *Neuron.* 37:953–962.

Proks, P., J.F. Antcliff, and F.M. Ashcroft. 2003. The ligand-sensitive gate of a potassium channel lies close to the selectivity filter. *EMBO Rep.* 4:70–75.

Qin, F., A. Auerbach, and F. Sachs. 1996. Estimating single-channel kinetic parameters from idealized patch-clamp data containing missed events. *Biophys. J.* 70:264–280.

Silberberg, S.D., A. Lagrutta, J.P. Adelman, and K.L. Magleby. 1996. Wanderlust kinetics and variable Ca^{2+}-sensitivity of *dslo*, a large conductance Ca^{2+}-activated K^+ channel, expressed in oocytes. *Biophys. J.* 70:2640–2651.

Solaro, C.R., J.P. Ding, Z.W. Li, and C.J. Lingle. 1997. The cytosolic inactivation domains of BKi channels in rat chromaffin cells do not behave like simple, open-channel blockers. *Biophys. J.* 73:819–830.

Toro, L., M. Ottolia, E. Stefani, and R. Latorre. 1994. Structural determinants in the interaction of Shaker inactivating peptide and a Ca^{2+}-activated K^+ channel. *Biochemistry.* 33:7220–7228.

Toro, L., E. Stefani, and R. Latorre. 1992. Internal blockade of a Ca^{2+}-activated K^+ channel by Shaker B inactivating "ball" peptide. *Neuron.* 9:237–245.

Wallner, M., P. Meera, and L. Toro. 1999. Molecular basis of fast inactivation in voltage and Ca^{2+}-activated K^+ channels: a transmembrane β-subunit homolog. *Proc. Natl. Acad. Sci. USA.* 96:4137–4142.

Webster, S.M., D. Del Camino, J.P. Dekker, and G. Yellen. 2004. Intracellular gate opening in Shaker K^+ channels defined by high-affinity metal bridges. *Nature.* 428:864–868.

Wilkens, C.M., and R.W. Aldrich. 2006. State independent block of BK channels by intracellular quaternary ammonium. *J. Gen. Physiol.* 128:347–364.

Xia, X.M., J.P. Ding, and C.J. Lingle. 1999. Molecular basis for the inactivation of Ca^{2+}- and voltage-dependent BK channels in adrenal chromaffin cells and rat insulinoma tumor cells. *J. Neurosci.* 19:5255–5264.

Xia, X.M., J.P. Ding, and C.J. Lingle. 2003. Inactivation of BK channels by the NH_2 terminus of the β2 auxiliary subunit: an essential role of a terminal peptide segment of three hydrophobic residues. *J. Gen. Physiol.* 121:125–148.

Xiao, J., X.G. Zhen, and J. Yang. 2003. Localization of PIP2 activation gate in inward rectifier K^+ channels. *Nat. Neurosci.* 6:811–818.

Yeh, J.Z., and C.M. Armstrong. 1978. Immobilisation of gating charge by a substance that simulates inactivation. *Nature.* 273:387–389.

Yellen, G., D. Sodickson, T.Y. Chen, and M.E. Jurman. 1994. An engineered cysteine in the external mouth of a K^+ channel allows inactivation to be modulated by metal binding. *Biophys. J.* 66:1068–1075.

Zagotta, W.N., T. Hoshi, and R.W. Aldrich. 1990. Restoration of inactivation in mutants of Shaker potassium channels by a peptide derived from ShB. *Science.* 250:568–571.

Zei, P.C., E.M. Ogielska, T. Hoshi, and R.W. Aldrich. 1999. Effects on ion permeation with hydrophobic substitutions at a residue in Shaker S6 that interacts with a signature sequence amino acid. *Ann. NY Acad. Sci.* 868:458–464.

Zheng, J., and F.J. Sigworth. 1998. Intermediate conductances during deactivation of heteromultimeric Shaker potassium channels. *J. Gen. Physiol.* 112:457–474.

Zhou, M., J.H. Morais-Cabral, S. Mann, and R. MacKinnon. 2001. Potassium channel receptor site for the inactivation gate and quaternary amine inhibitors. *Nature.* 411:657–661.